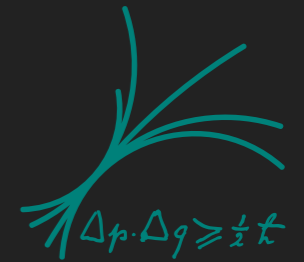




MAX-PLANCK-GESELLSCHAFT



Max-Planck-Institut für Physik
(Werner-Heisenberg-Institut)

DIELECTRIC HALOSCOPE AND

THE EXPERIMENT

XIAOYUE LI

MAX PLANCK INSTITUTE FOR PHYSICS
AXION COSMOLOGY, MIAPP, GARCHING

FEB. 18, 2020

THE STRONG CP PROBLEM

- ▶ The QCD Lagrangian contains a CP-violating term:

$$\mathcal{L}_{QCD} = \dots + \frac{\alpha_s}{8\pi} \bar{\theta} G_{\mu\nu a} \tilde{G}_a^{\mu\nu}, \quad \bar{\theta} = \theta_{QCD} + \theta_{Yukawa} \in [-\pi, \pi] \sim \mathcal{O}(1)$$

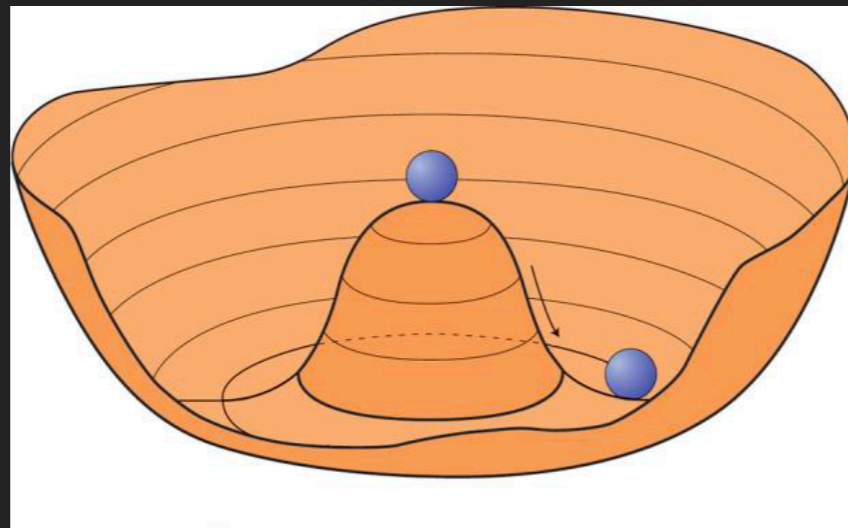
- ▶ Neutron electric dipole moment

$$d_N \sim 10^{-16} \bar{\theta} \text{ e-cm} < 3 \times 10^{-26} \text{ e-cm} \Rightarrow \bar{\theta} < 3 \times 10^{-10}$$

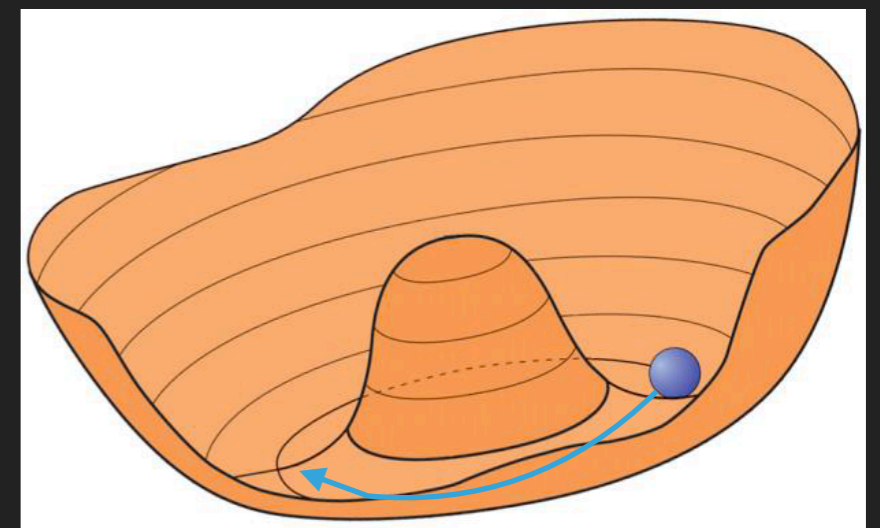
- ▶ The Standard Model does not provide a reason for why $\bar{\theta}$ is so tiny, i.e. the strong CP problem.
- ▶ The Peccei-Quinn mechanism provides a reason for the value of $\bar{\theta}$ and predicts a light neutral pseudoscalar boson – the axion.

THE PECCEI-QUINN MECHANISM

- ▶ Peccei-Quinn introduces a global $U(1)_{PQ}$ symmetry which spontaneously breaks at $T = f_a \gg \Lambda_{QCD}$

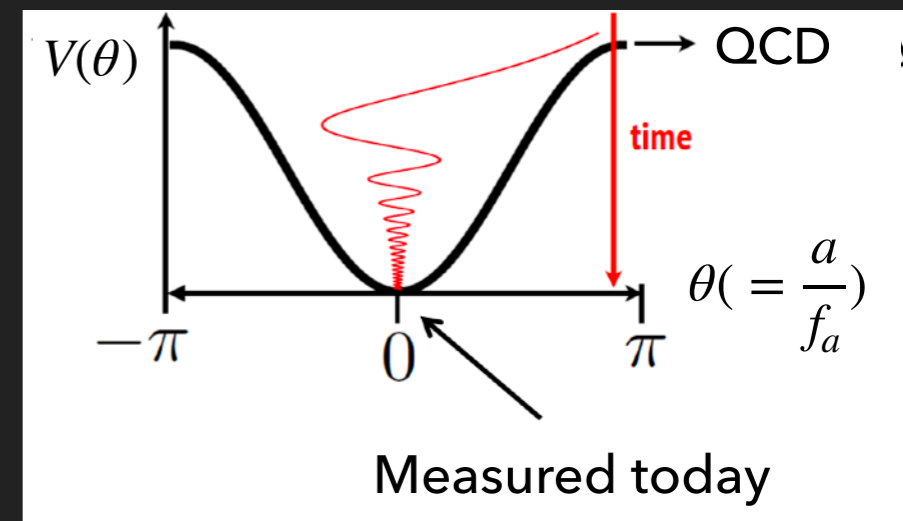


$1 \text{ GeV} < T < f_a$ (PQ symmetry breaking)

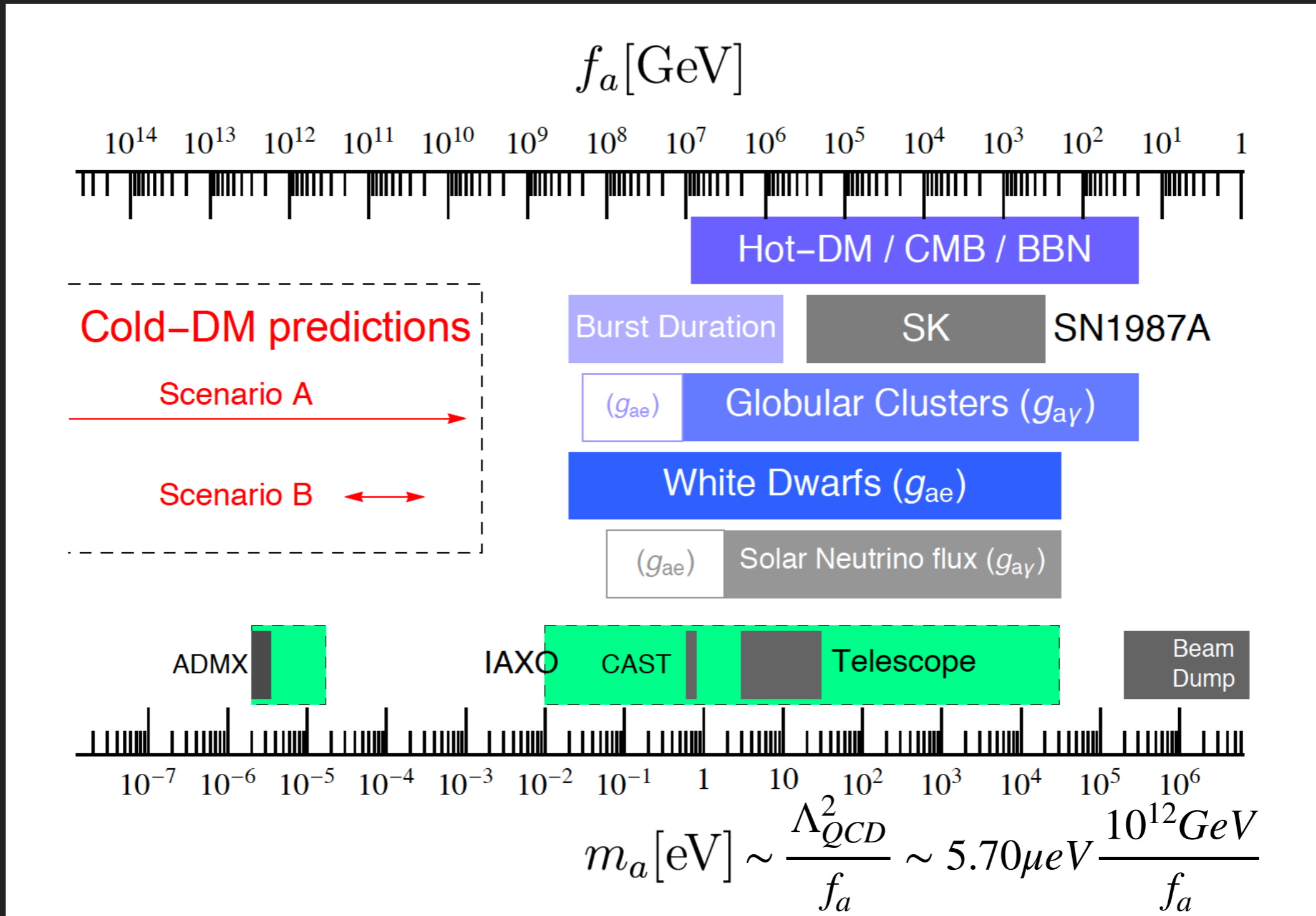


$T < 1 \text{ GeV}$ (QCD phase transition)

- ▶ $\mathcal{L} = \dots + \bar{\theta} \frac{\alpha_s}{8\pi} G_{\mu\nu a} \tilde{G}_a^{\mu\nu} + \frac{1}{2} \partial_\mu a \partial^\mu a + \frac{a}{f_a} \frac{\alpha_s}{8\pi} G_{\mu\nu a} \tilde{G}_a^{\mu\nu}$
- ▶ Axion potential $V_a(a/f_a)$ is minimized at $\bar{\theta} + \frac{a}{f_a} = 0$
- ▶ The axions produced by the "misalignment" mechanism are a good CDM candidate



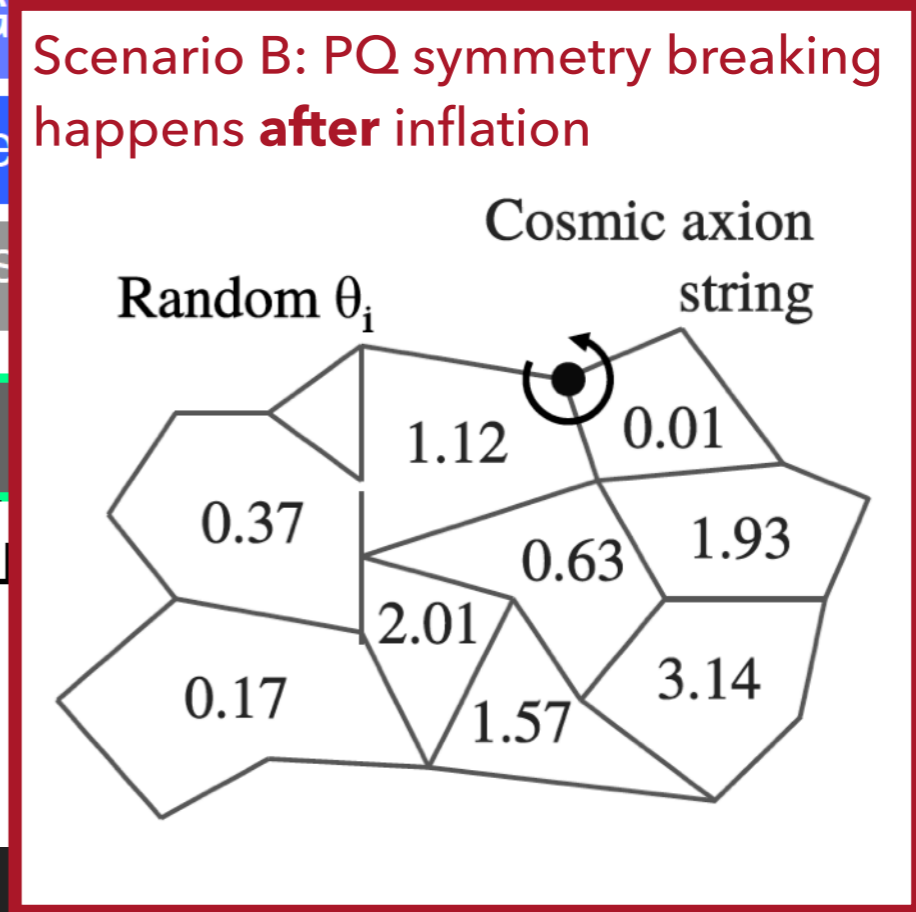
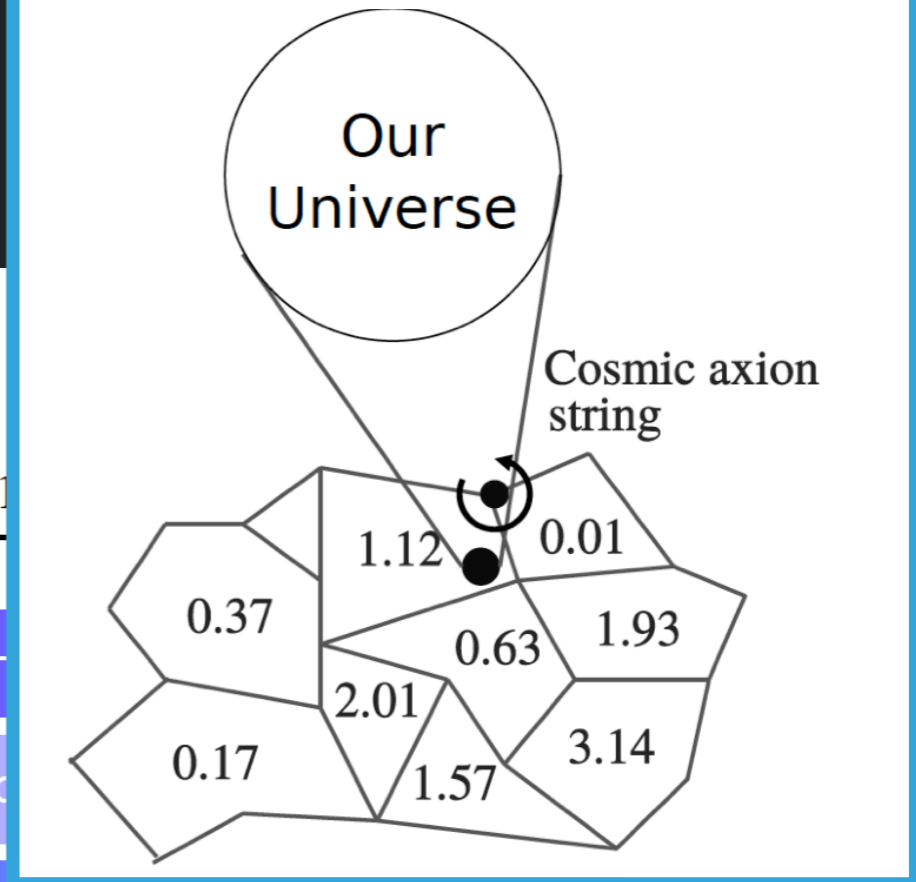
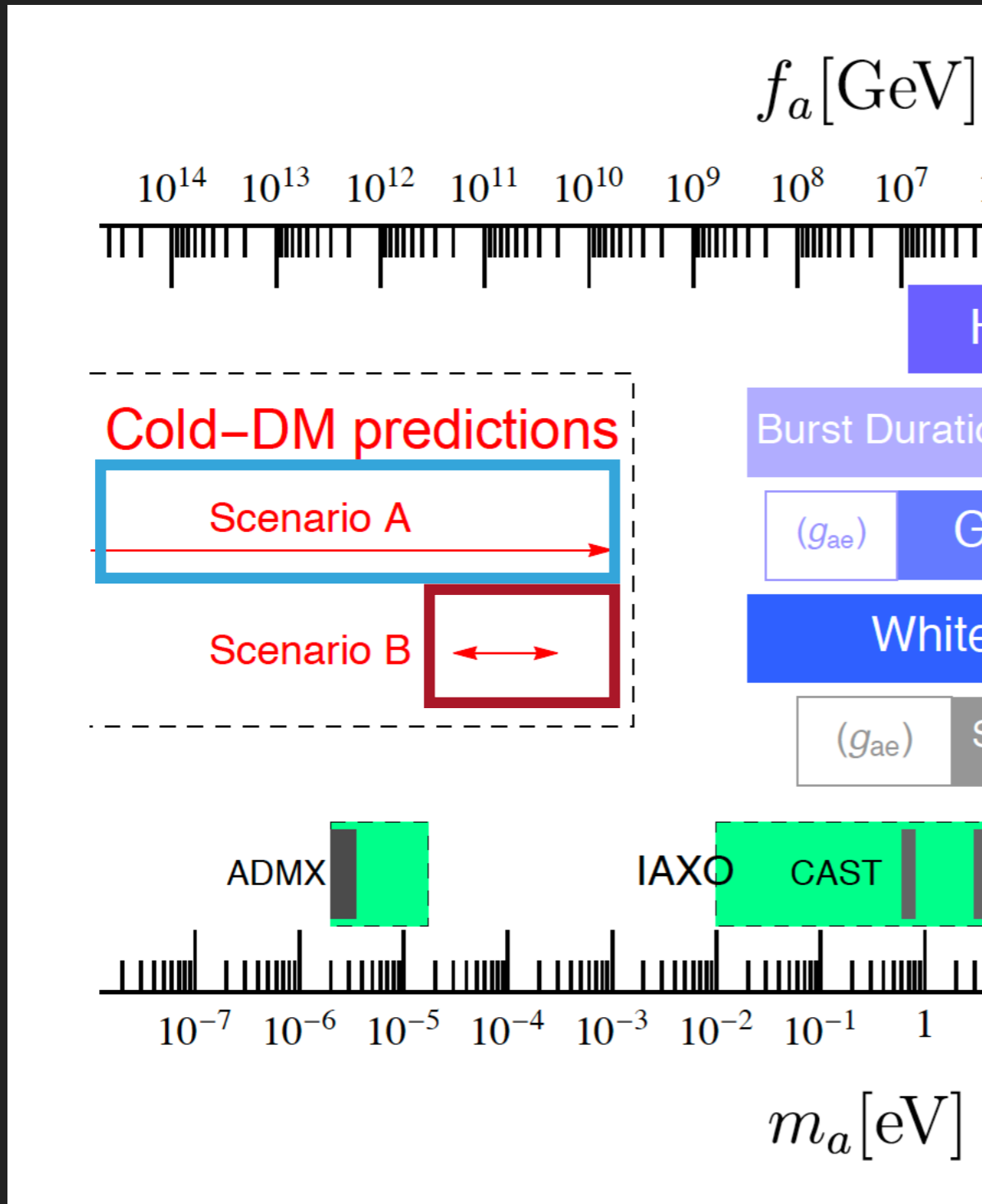
CONSTRAINTS ON QCD AXION MASS





Scenario A: PQ symmetry breaking happens **before** inflation

CONSTRAINTS ON QCD AXION MASS



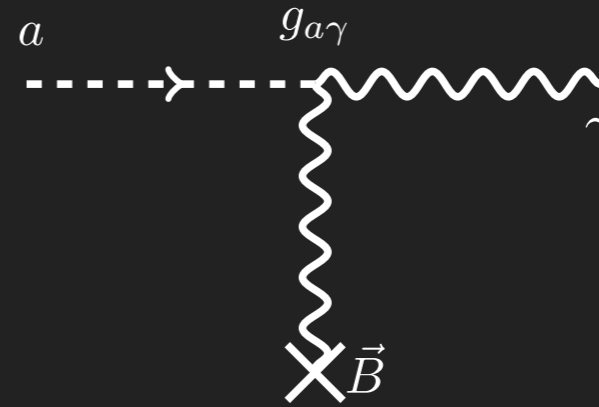
CDM AXION DIRECT-DETECTION

- ▶ Axion-photon interaction:

$$\mathcal{L}_{a\gamma\gamma} = C_{a\gamma} \frac{\alpha}{2\pi f_a} a F^{\mu\nu} \tilde{F}_{\mu\nu}$$

↓

$$g_{a\gamma} = 2.04(3) \times 10^{-16} \text{GeV}^{-1} \frac{m_a}{\mu\text{eV}} C_{a\gamma}$$



- ▶ CDM axions behave like a **classical wave**: $a/f_a = \theta = \theta_0 \cos(m_a t)$

- ▶ E.g. $m_a \sim 100 \mu\text{eV}$, local galactic axion density $\rho_a = (f_a m_a)^2 \theta_0^2 / 2 = 0.45 \text{ GeV}/\text{cm}^3$

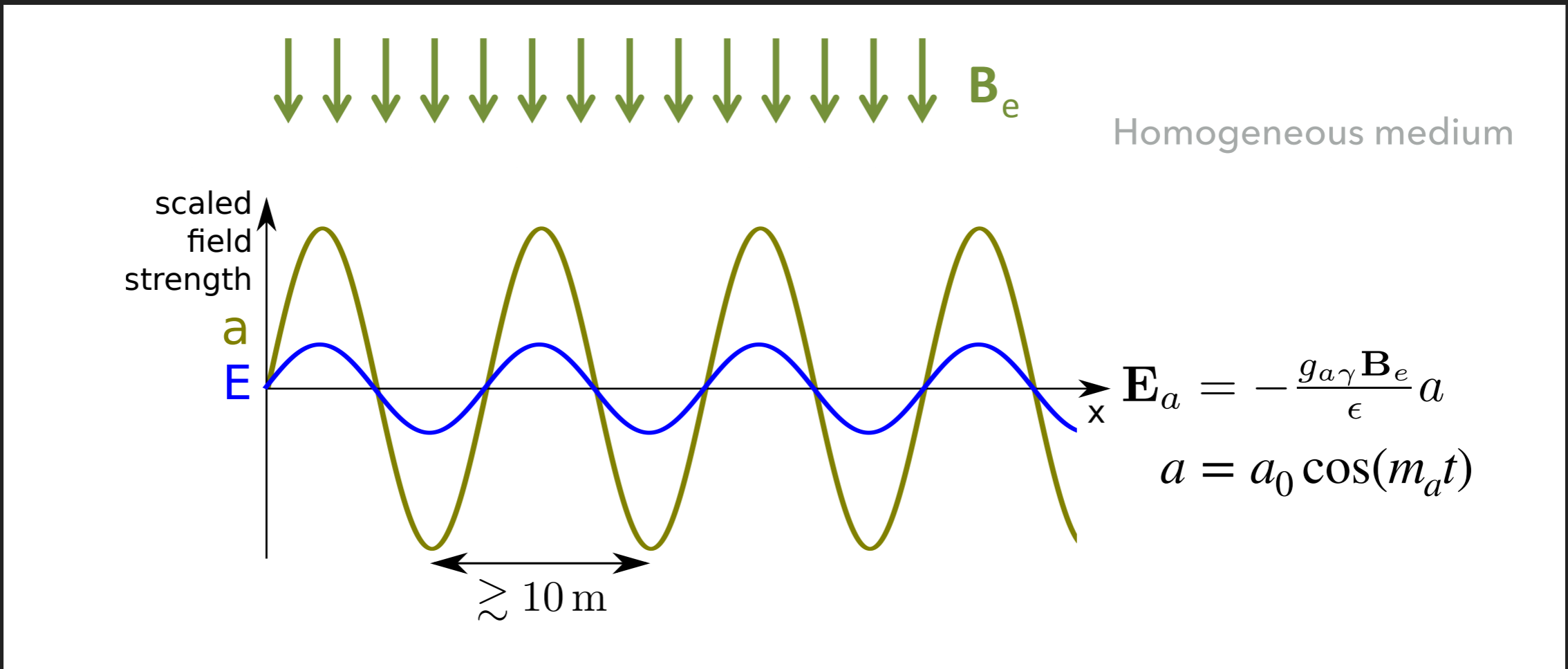
- ▶ Axion de Broglie wavelength: $\lambda_a = \frac{2\pi}{m_a v_a} \gtrsim 10 \text{ m}$ ($v_a \approx 10^{-3} c$)

- ▶ Axion phase-space occupancy: $\mathcal{N}_a \sim n_a \lambda_a^3 = (\rho_a / m_a) \lambda_a^3 \sim 10^{22}$

- ▶ **Macroscopic** axion-Maxwell equation under external B-field:

$$\begin{cases} \nabla \cdot \mathbf{D} = \rho_f - g_{a\gamma} \mathbf{B}_e \cdot \nabla a \\ \nabla \times \mathbf{H} - \dot{\mathbf{D}} = \mathbf{J}_f + g_{a\gamma} \mathbf{B}_e \dot{a} \end{cases}$$

AXION HALOSCOPE

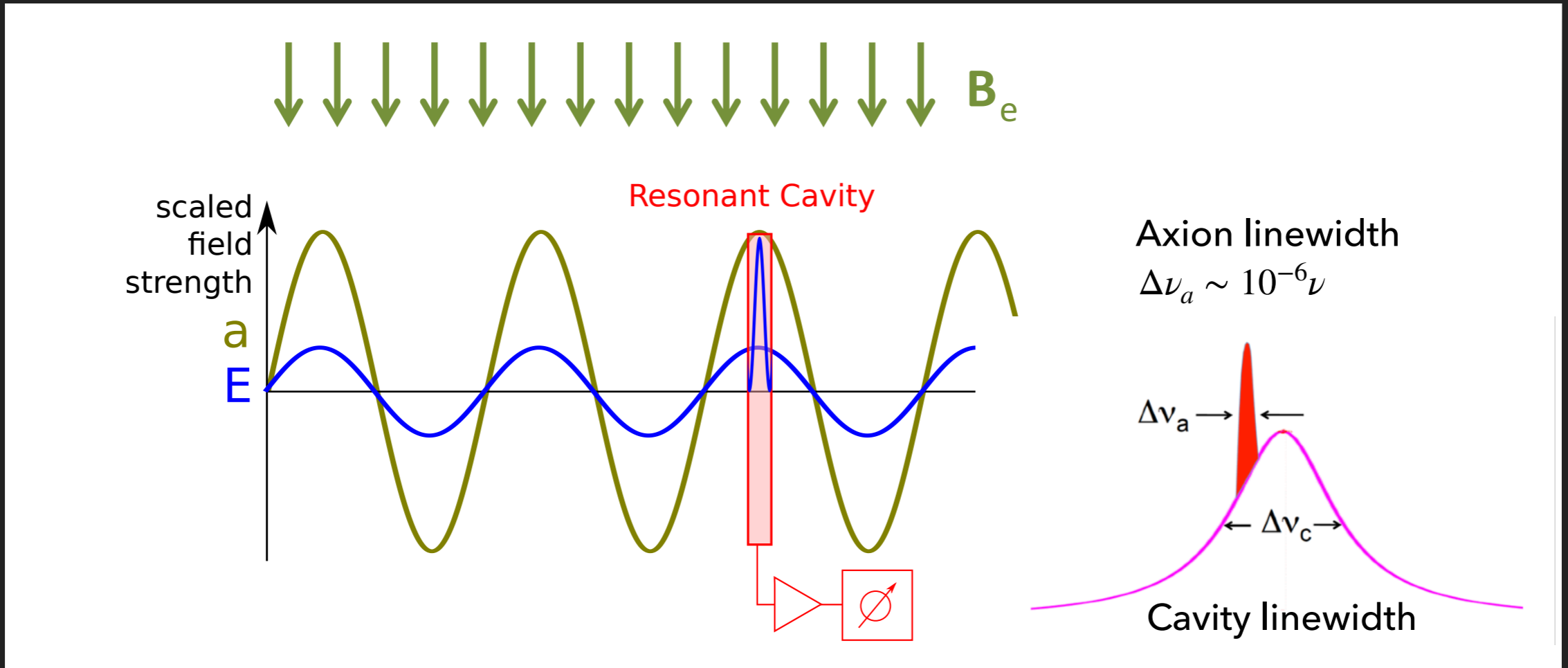


▶ Axion induced electric field:

$$|\mathbf{E}_a| = \left| -\frac{g_{a\gamma}\mathbf{B}_e}{\epsilon}a \right| = 1.3 \times 10^{-12} \text{ Vm}^{-1} \times \left(\frac{B_e}{10 \text{ T}} \right) \left(\frac{\rho_a}{300 \text{ MeV/cm}^3} \right)^{1/2} \frac{C_{a\gamma}}{\epsilon}$$

↗ Local axion DM density
↘ Dielectric constant

CAVITY HALOSCOPE

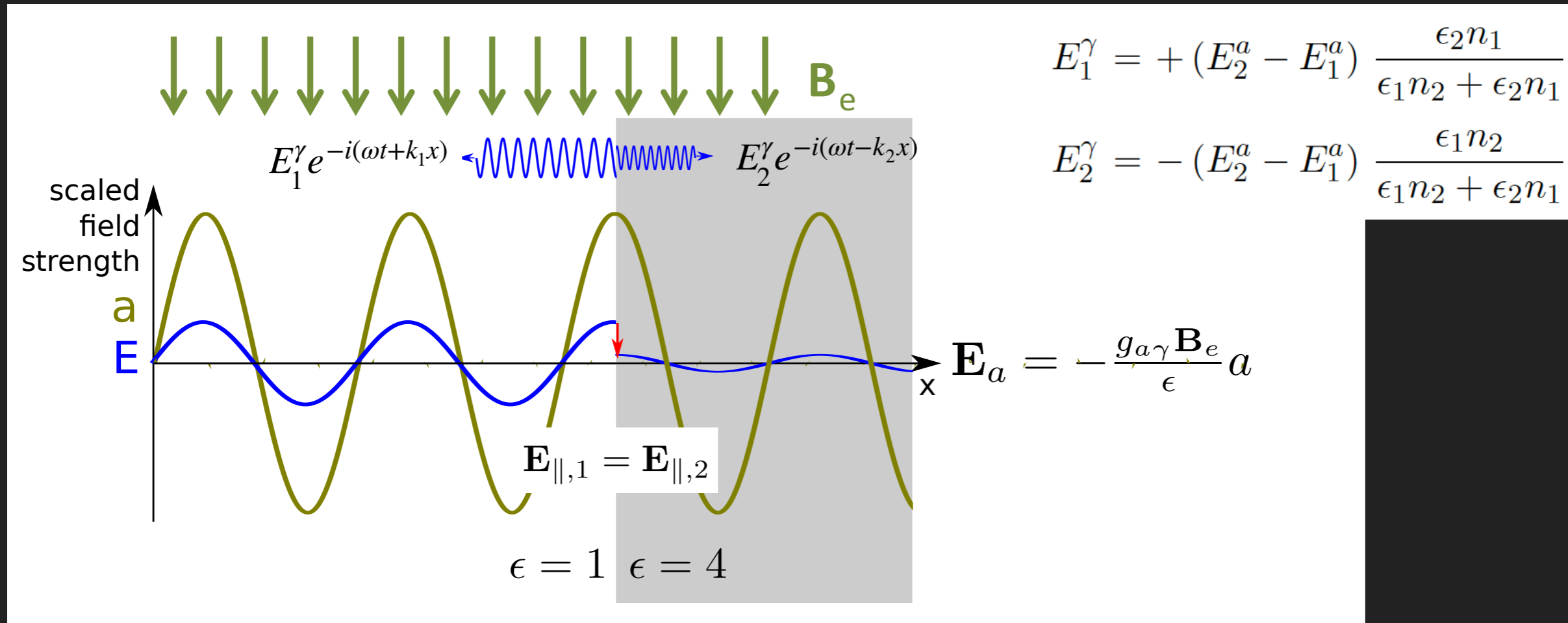


$$P_{sig} \sim 1.9 \times 10^{-22} \text{ W} \left(\frac{V}{136l} \right) \left(\frac{B_e}{6.8T} \right)^2 \left(\frac{C}{0.4} \right) \left(\frac{C_{a\gamma\gamma}}{0.97} \right)^2 \left(\frac{\rho_a}{0.45 \text{ GeV cm}^{-3}} \right) \left(\frac{f}{650 \text{ MHz}} \right) \left(\frac{Q}{50,000} \right)$$

Cavity volume, scaled by f^{-3}
Cavity form factor
Cavity Quality factor

► At higher frequencies, cavities are increasingly difficult to build

DIELECTRIC HALOSCOPE (1)

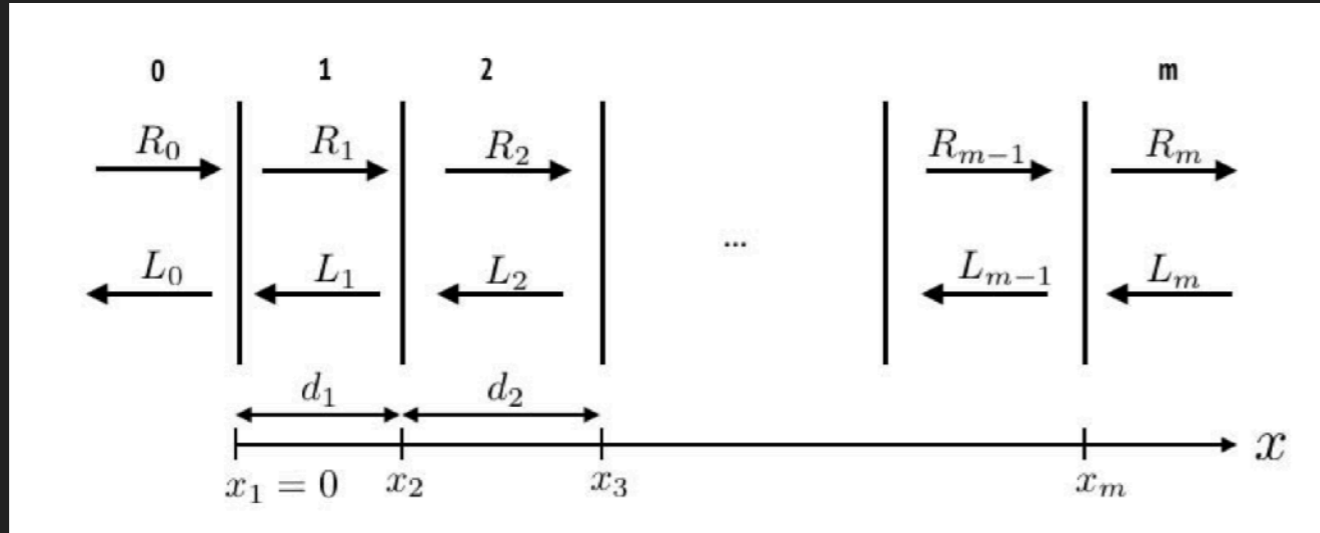


► Power emitted at a vacuum-to-perfect-conductor interface:

$$\frac{P_{sig}^\gamma}{A} = 2.2 \times 10^{-27} \frac{\text{W}}{\text{m}^2} \left(\frac{B_e}{10 \text{ T}} \right)^2 C_{a\gamma}^2$$

DIELECTRIC HALOSCOPE (2)

"Axion-photon conversion caused by dielectric interfaces: quantum field calculation", A. N. Ioannisian, N. Kazarian, A. J. Millar, G G. Raffelt, DOI: 10.1088/1475-7516/2017/09/005



► In the r^{th} domain

$$E_a^r = -A_r E_0,$$

$$\text{where } A_r = \frac{1}{\epsilon_r} \frac{B_{e,r}}{B_{e,max}},$$

$$E_0 = g_{a\gamma} B_{e,max} a_0$$

► Continuity conditions at each boundary

$$\begin{pmatrix} R_{r+1} \\ L_{r+1} \end{pmatrix} = G_r P_r \begin{pmatrix} R_r \\ L_r \end{pmatrix} + E_0 S_r \begin{pmatrix} 1 \\ 1 \end{pmatrix}, \text{ where}$$

$$G_r = \frac{1}{2n_r + 1} \begin{pmatrix} n_{r+1} + n_r & n_{r+1} - n_r \\ n_{r+1} - n_r & n_{r+1} + n_r \end{pmatrix},$$

$$P_r = \begin{pmatrix} e^{i\delta_r} & 0 \\ 0 & e^{-i\delta_r} \end{pmatrix},$$

$$S_r = \frac{A_{r+1} - A_r}{2} \begin{pmatrix} 1 & 0 \\ 0 & 1 \end{pmatrix}$$

Transfer matrix between
in and out EM waves

Axion source terms

$$\begin{pmatrix} R_m \\ L_m \end{pmatrix} = T \begin{pmatrix} R_0 \\ L_0 \end{pmatrix} + E_0 M \begin{pmatrix} 1 \\ 1 \end{pmatrix}, \text{ where}$$

$$T_a^b = G_{a-1} P_{a-1} G_{a-2} P_{a-2} \cdots G_{b+1} P_{b+1} G_b P_b,$$

$$T = T_0^m, \text{ and}$$

$$M = \sum_{s=1}^m T_s^m S_{s-1}$$

DIELECTRIC HALOSCOPE (3)

- ▶ A perfect mirror on the left

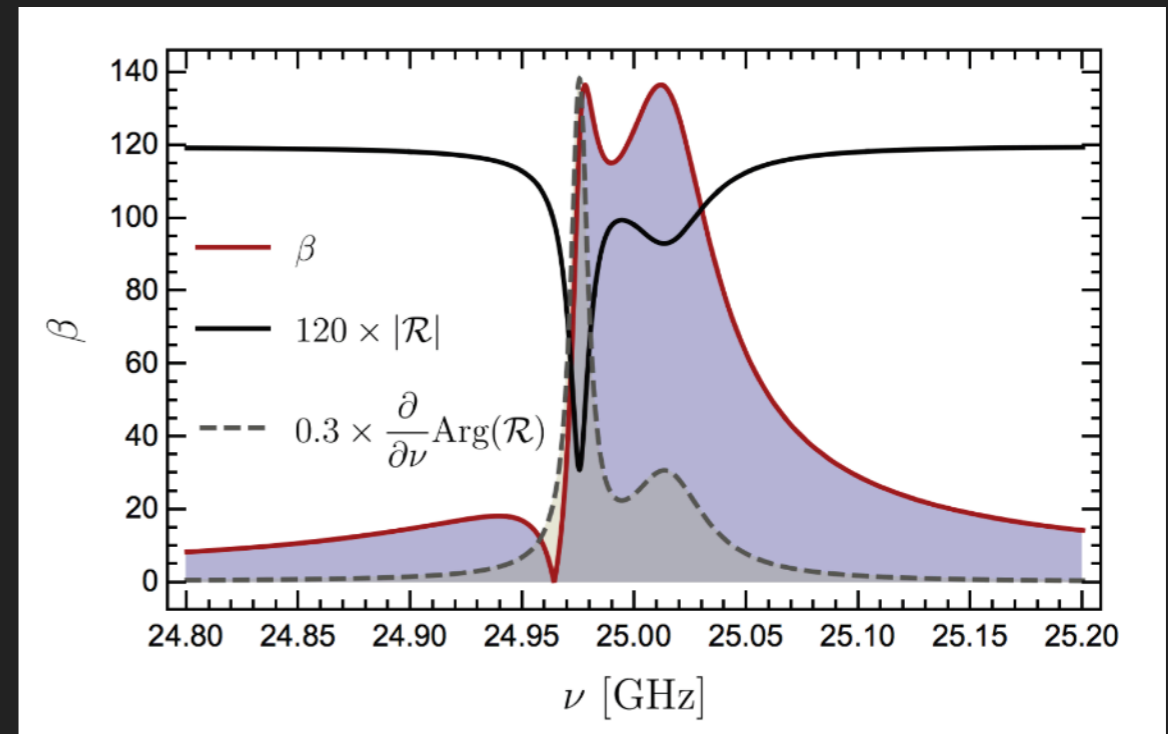
$$\text{Reflectivity } R_R = \frac{R_m}{L_m} \Big|_{R_0=0} = \frac{T[1,2]}{T[2,2]}$$

$$\text{Boost } \beta = \frac{R_m}{E_0} = M[1,1] + M[1,2]$$

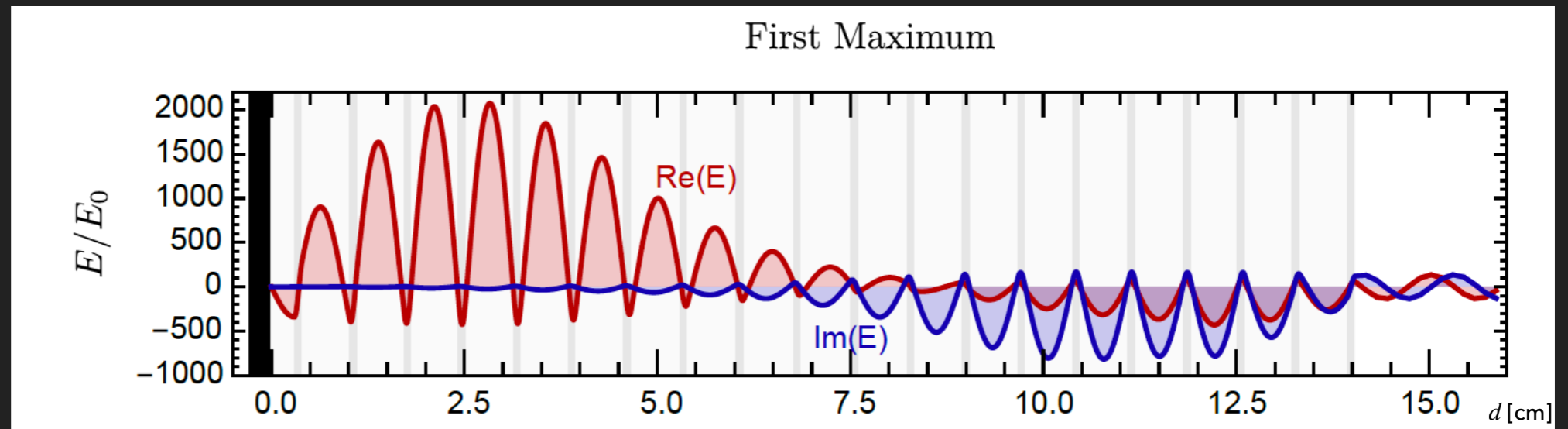
- ▶ Tolerance to disc positioning inaccuracy:

$$\sigma \ll 200 \mu\text{m} \left(\frac{10^2}{\beta} \right)^{1/2} \left(\frac{100 \mu\text{eV}}{m_a} \right)$$

20 discs, $d = 1 \text{ mm}$, $n = 5$

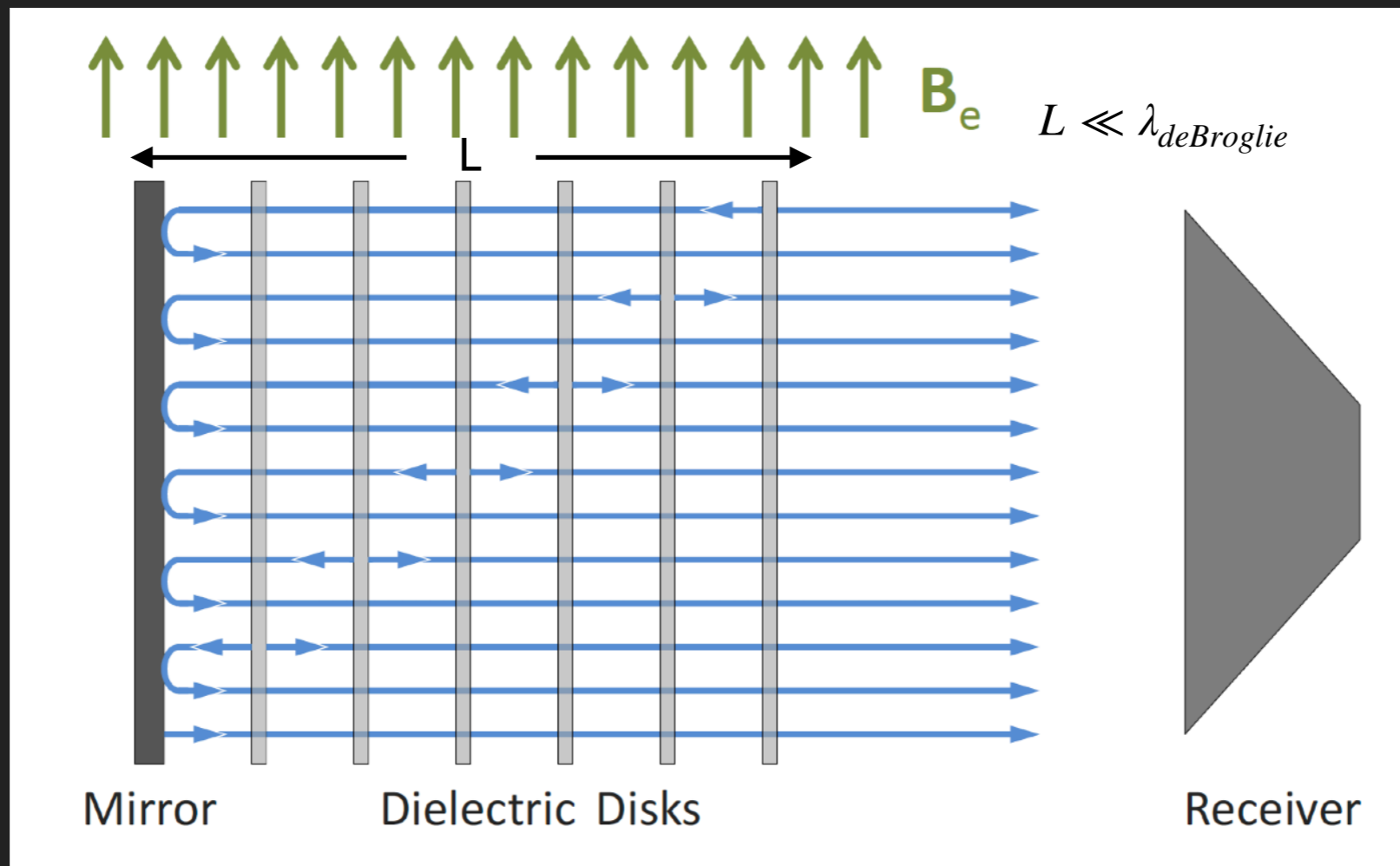


First Maximum



MAgnetized Disc and Mirror Axion eXperiment (MADMAX)

Cryogenic environment



- ▶ Power enhancement from coherent emission from and resonances between interfaces

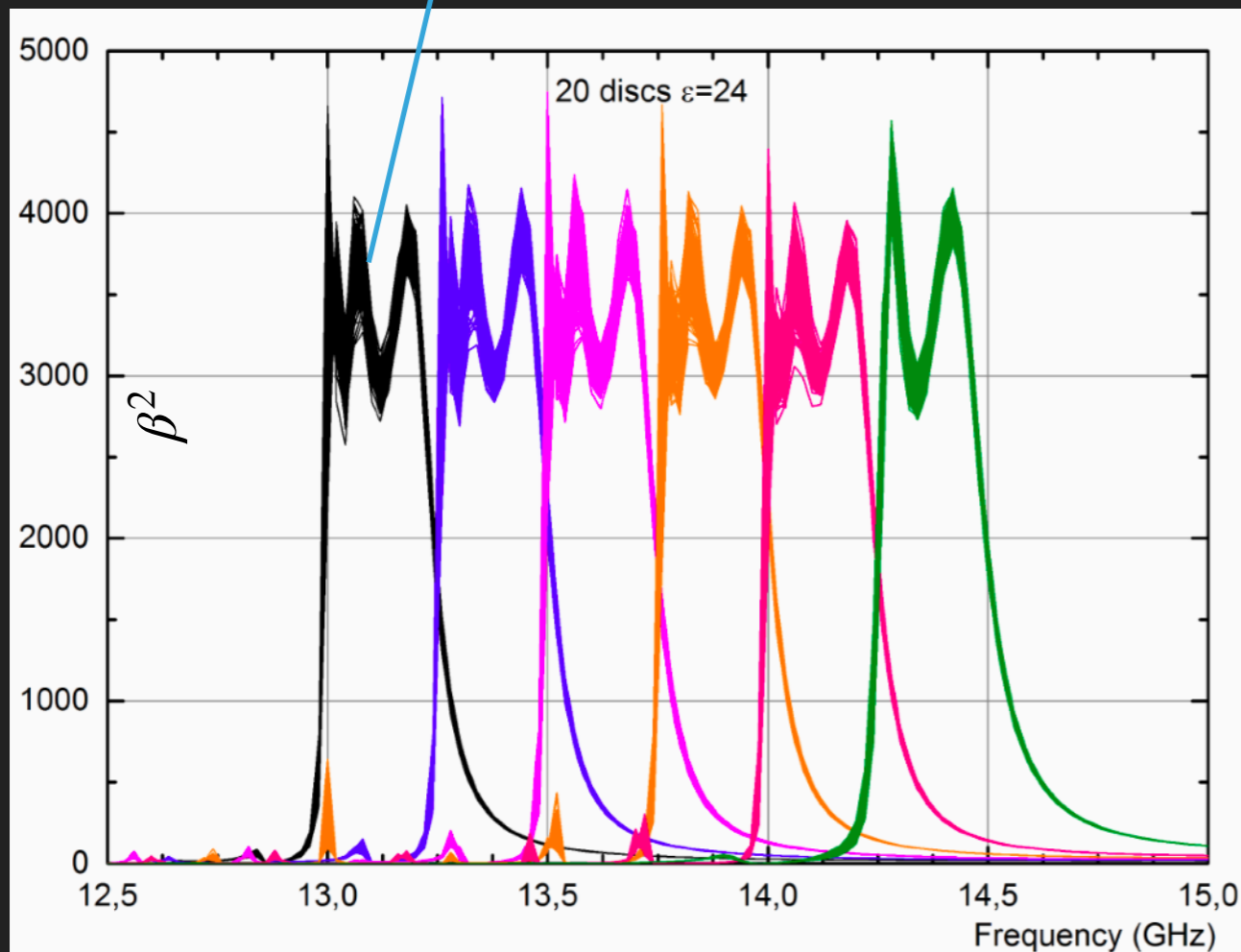
$$\frac{P_{sig}}{A} = 2.2 \times 10^{-27} \frac{\text{W}}{\text{m}^2} \left(\frac{B_e}{10 \text{ T}} \right)^2 C_{ay}^2 \cdot \beta^2 \longrightarrow \text{Boost factor } \beta^2 \geq 10^4 \text{ achievable}$$

$\sim \text{m}^2$ ←

MADMAX BOOST FACTOR

- ▶ Frequency tuning possible

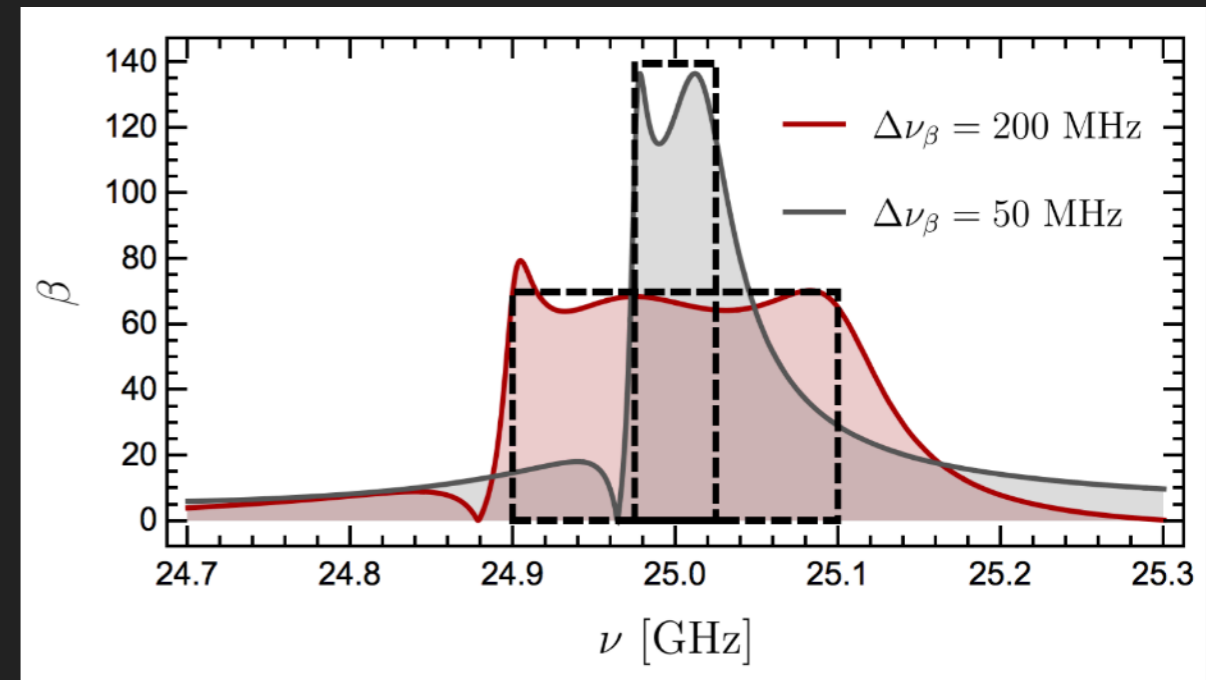
Disc positions randomly varied by $\sigma = 15 \mu\text{m}$



Frequency is tuned by changing disc positions

- ▶ Area law: $\int |\beta(\nu)|^2 d\nu \propto N$

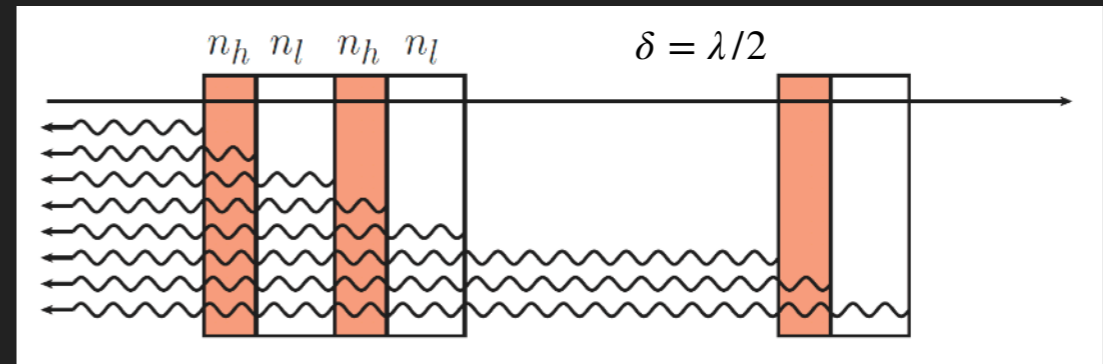
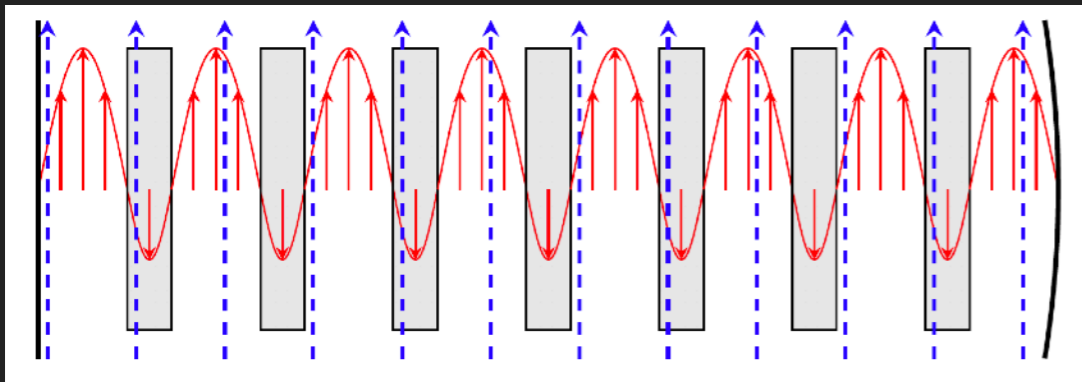
- ▶ Options for broadband and narrowband scans



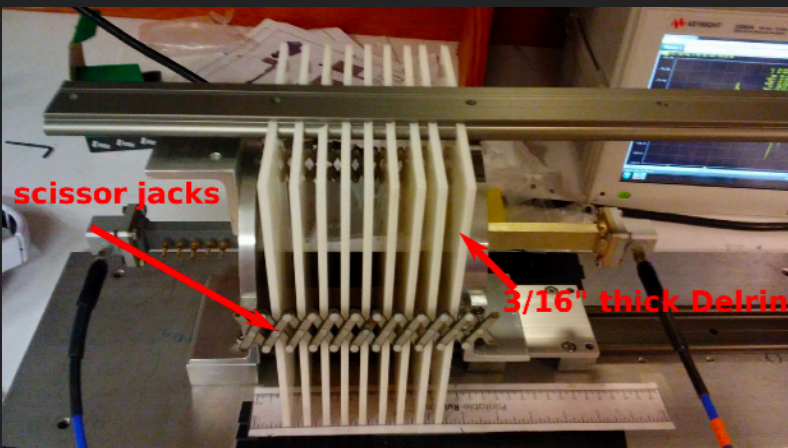
OTHER DIELECTRIC HALOSCOPES

J. Jaeckel, J. Redondo, DOI:10.1103/PhysRevD.88.115002

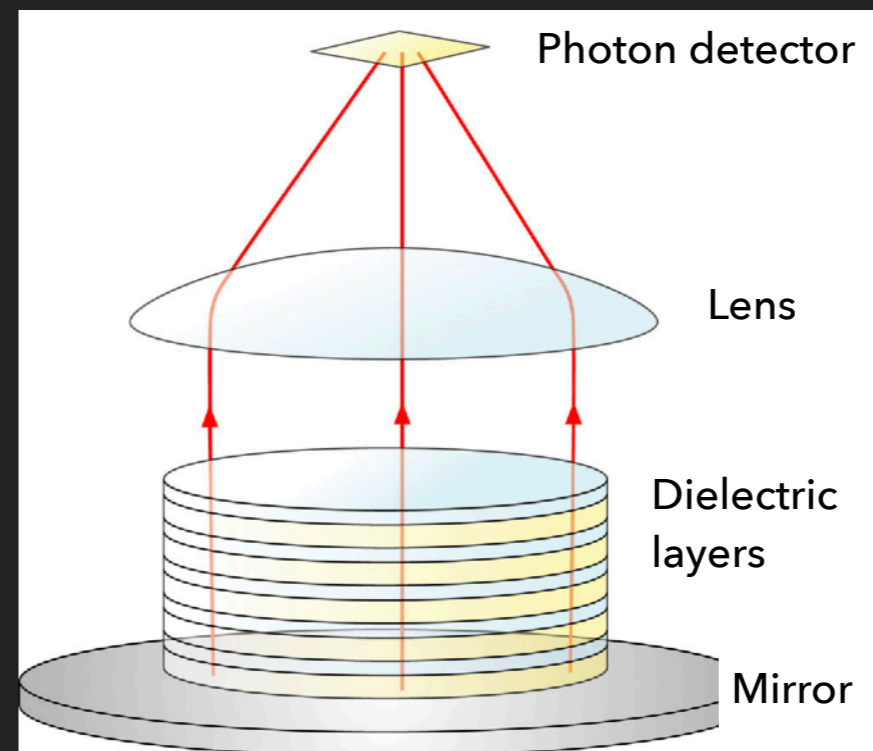
ADMX Orpheus



M. Baryakhtar, J. Huang, R. Lasenby, PRD 98, 035006 (2018)



15-18 GHz



Infrared to ultraviolet

- ▶ Open cavity with evenly spaced dielectrics
- ▶ Dielectric media compresses wavenumber and prevent the form factor integral from dropping to zero

YOU'RE TRYING TO PREDICT THE BEHAVIOR
OF <COMPLICATED SYSTEM>? JUST MODEL
IT AS A <SIMPLE OBJECT>, AND THEN ADD
SOME SECONDARY TERMS TO ACCOUNT FOR
<COMPLICATIONS I JUST THOUGHT OF>.

EASY, RIGHT?

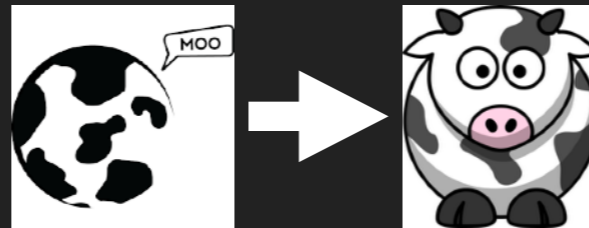
SO, WHY DOES <YOUR FIELD> NEED
A WHOLE JOURNAL, ANYWAY?



xkcd.com

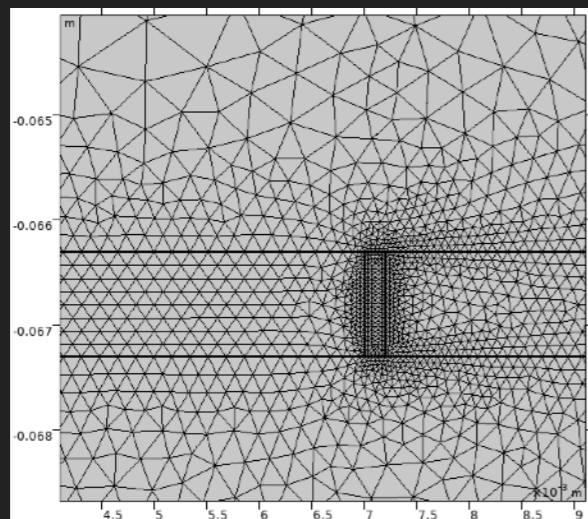
- ▶ More realistic simulations
- ▶ Frequency tuning in reality
- ▶ RF signal detection
- ▶ Other engineering challenges

3D SIMULATION (1)



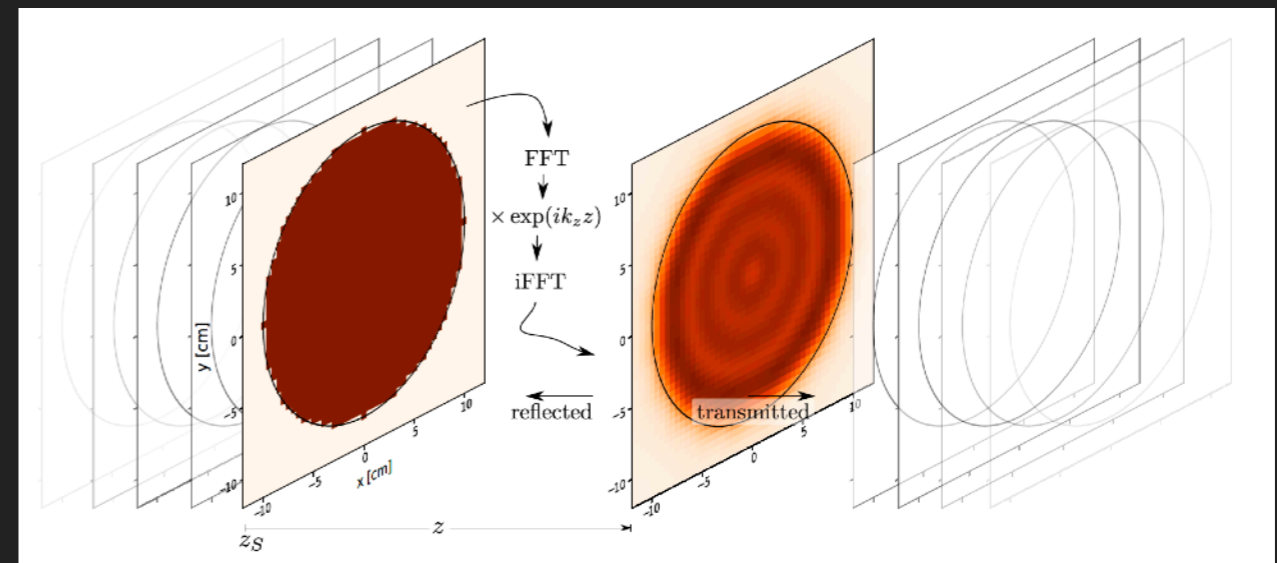
A. Finite element method (FEM) w/
Comsol Multiphysics [®] and Elmer

- ▶ Axion-induced E field is implemented as an external current density: $\mathbf{J}_a(t) = g_{a\gamma} \mathbf{B}_e \dot{a}(t)$
- ▶ Fewer underlying assumptions but time-consuming



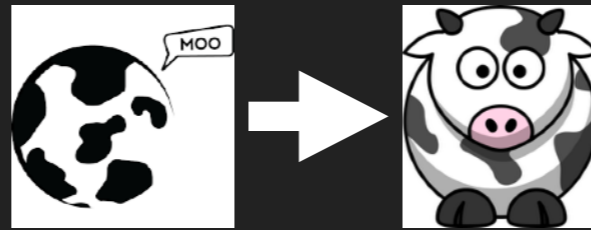
B. Recursive Fourier propagation method

- ▶ Assumption: no charge accumulation, i.e. $\nabla \cdot \mathbf{E} = 0$



$$E_i(\mathbf{x}) = \int_{\mathbb{R}^2} \frac{dk_x dk_y}{(2\pi)^2} \mathcal{F}(E_i)(k_x, k_y) \times e^{i|z-z_s| \sqrt{(\omega n)^2 - k_x^2 - k_y^2}} e^{ik_x x} e^{ik_y y}$$

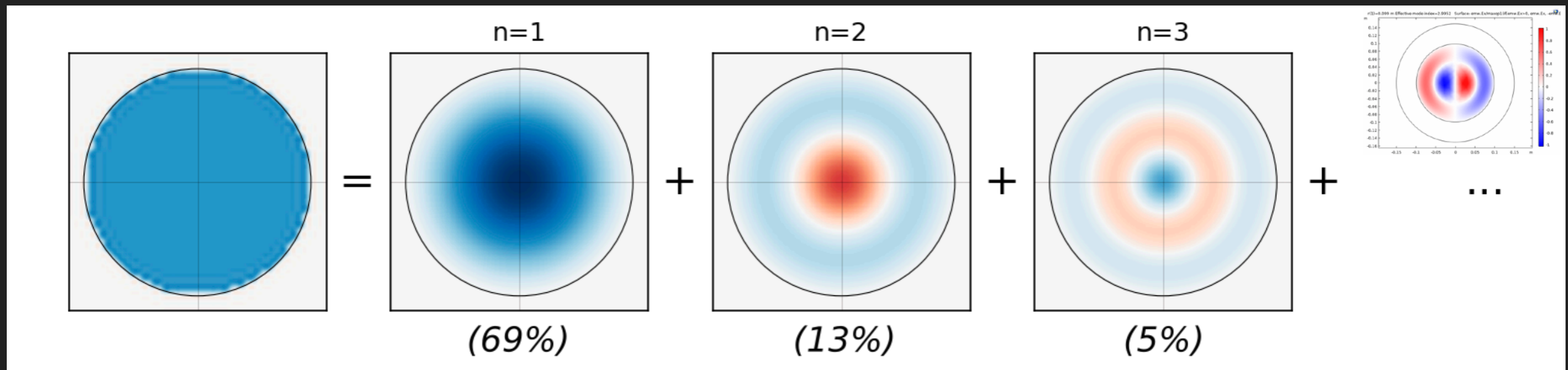
3D SIMULATION (2)



C. Mode matching

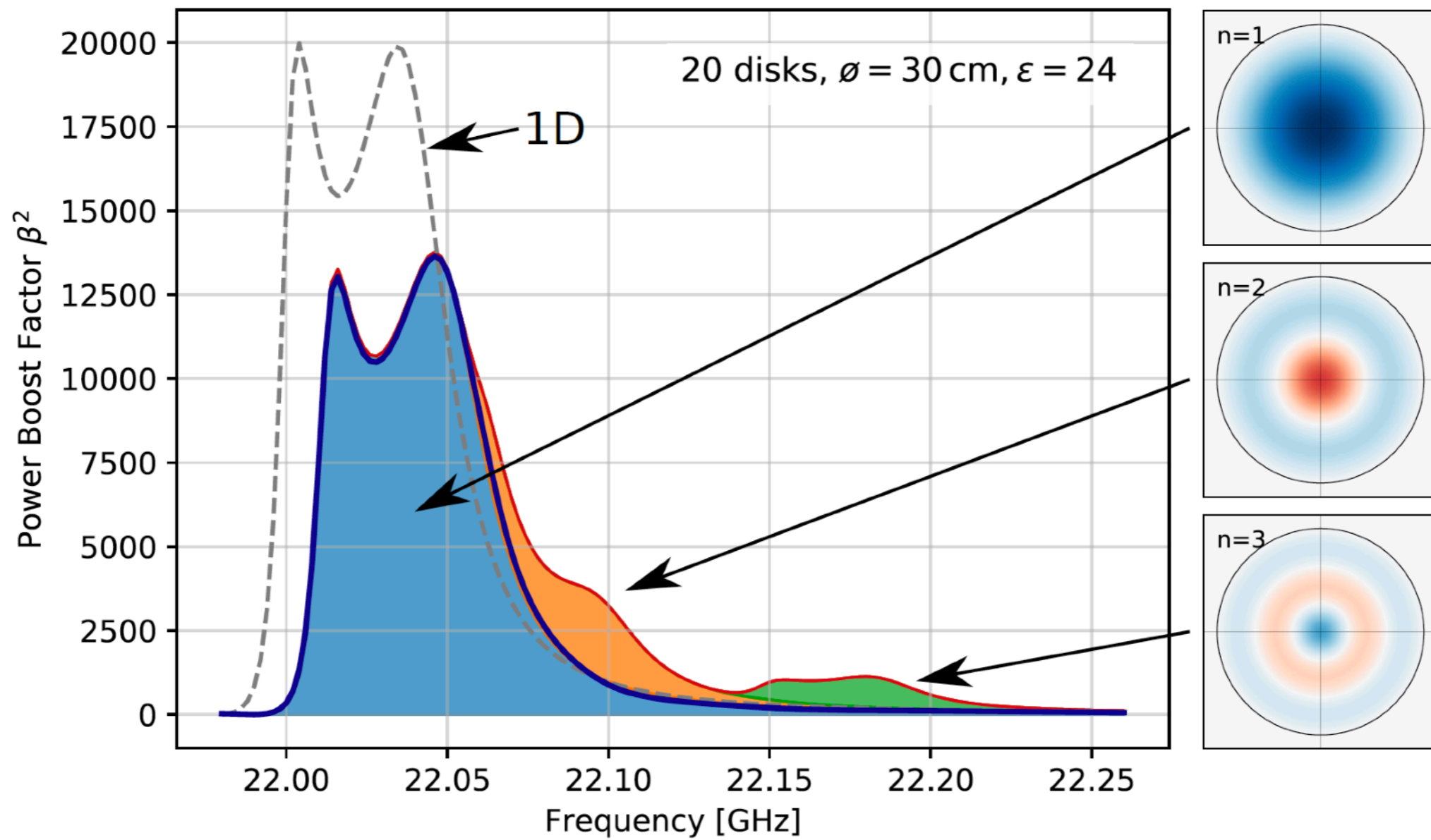
- ▶ If the booster mechanics have negligible effects, the booster can be regarded as similar to a dielectric waveguide

Eigenmodes w/ different field patterns and propagation constant



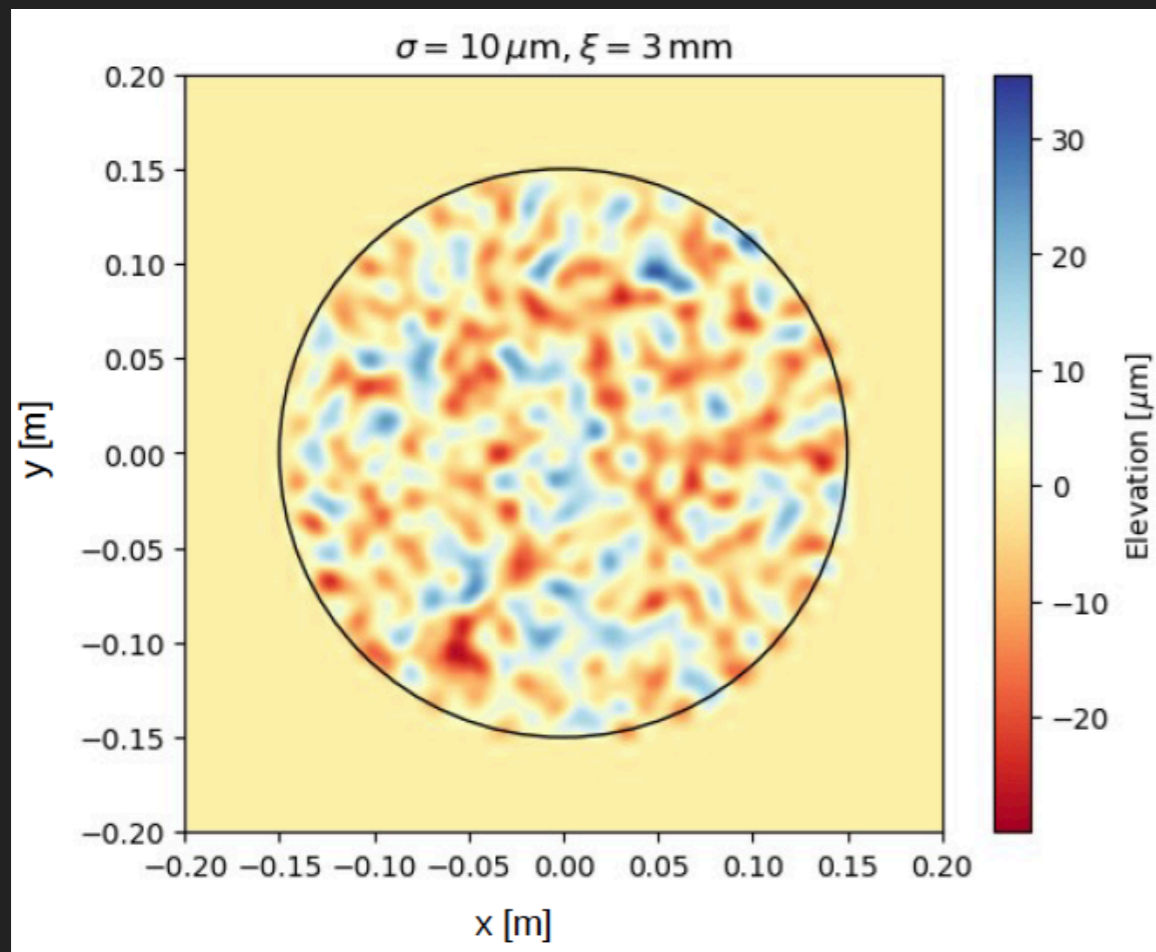
- ▶ Mode mixing can happen due to diffraction, tilted disc, etc.
- ▶ Three methods yield consistent results where comparison is possible

3D SIMULATION (3)

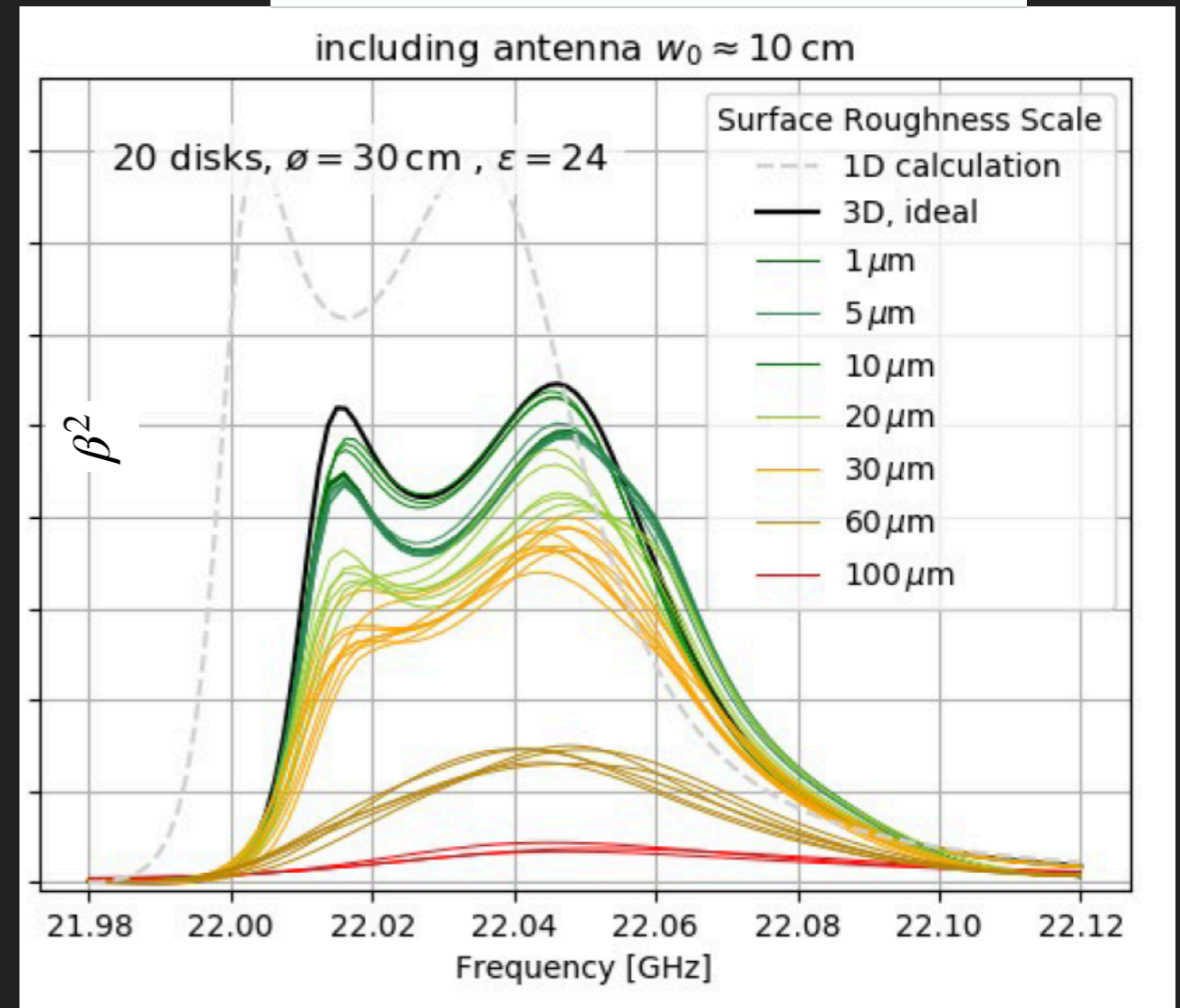
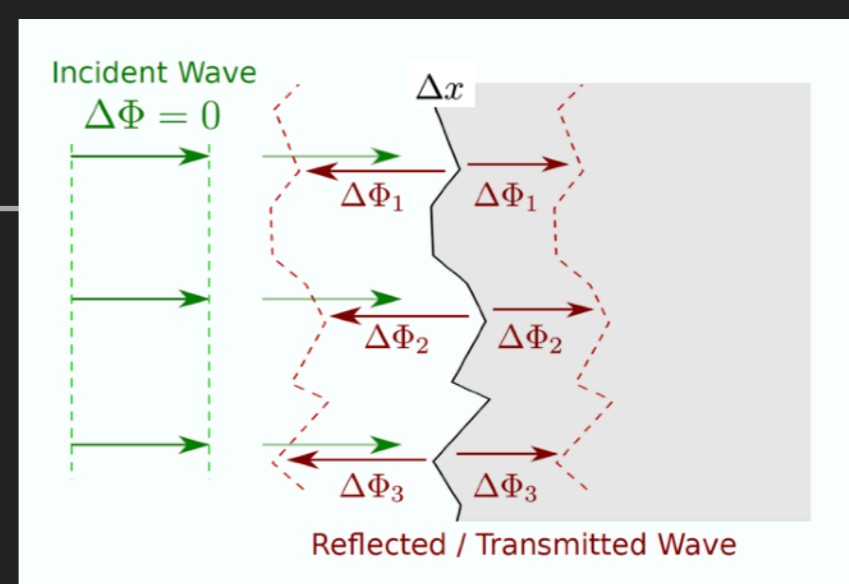


CRITICAL DESIGN PARAMETERS (1)

► Disc surface roughness



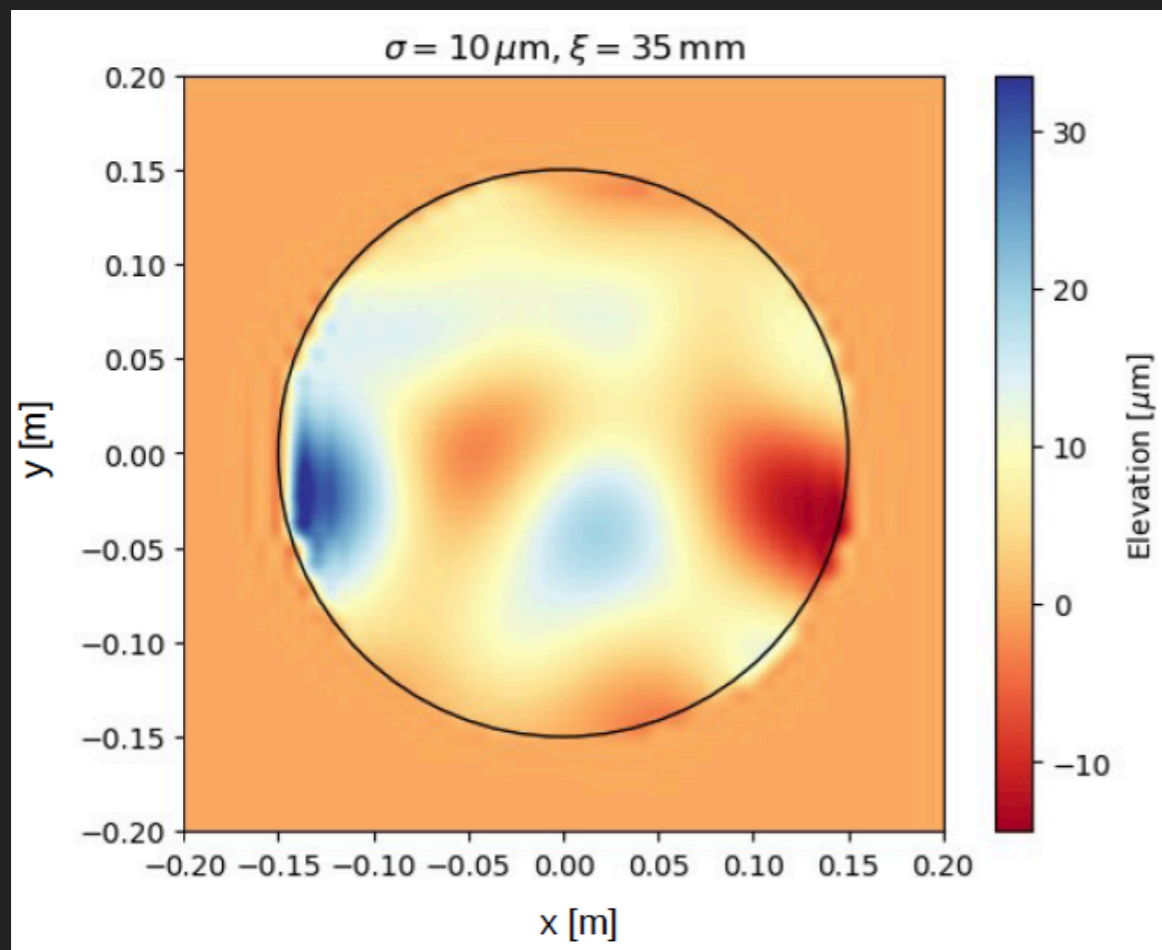
Correlation length 3 mm



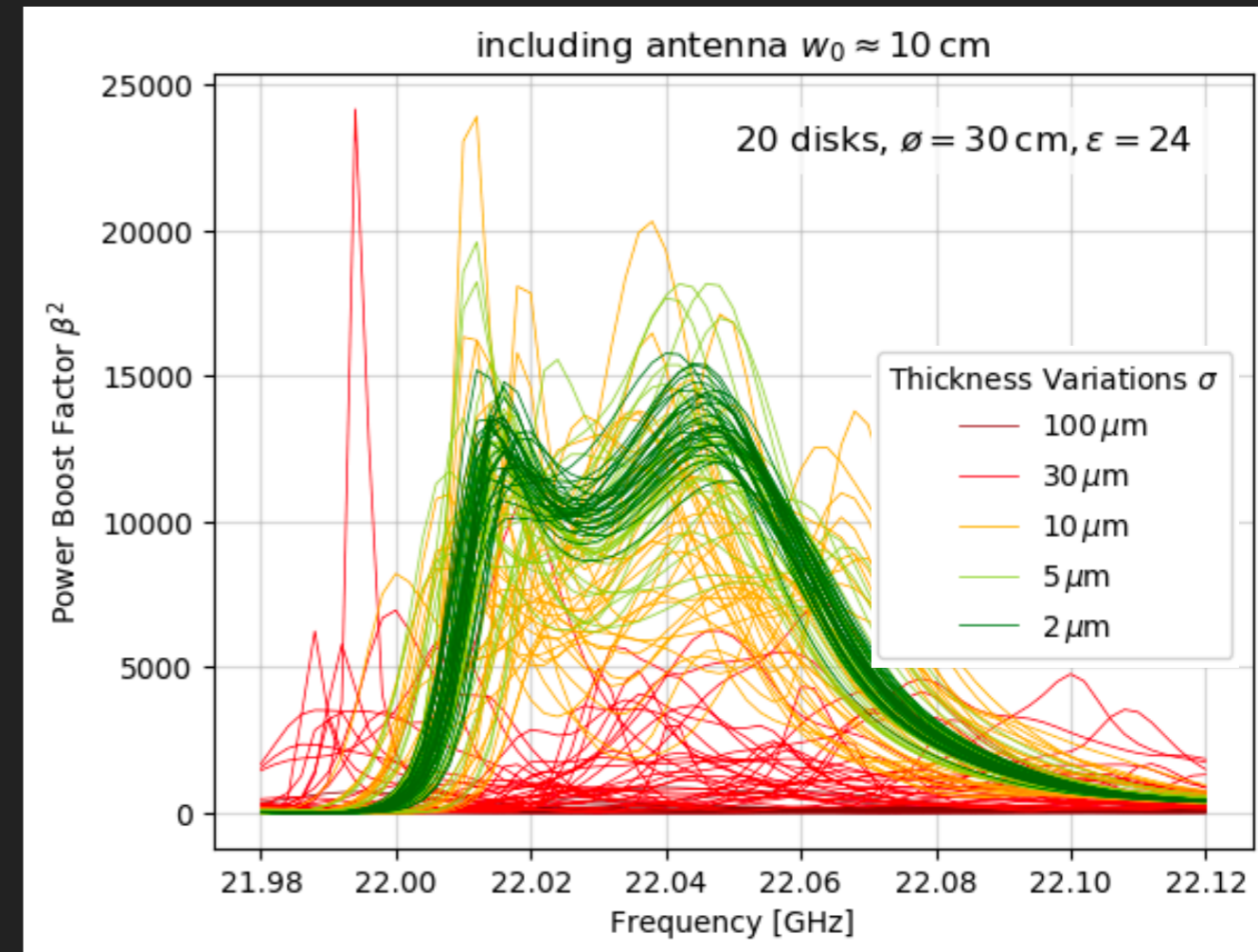
► Booster is forgiving to small-scale roughness

CRITICAL DESIGN PARAMETERS (2)

► Disc thickness variation

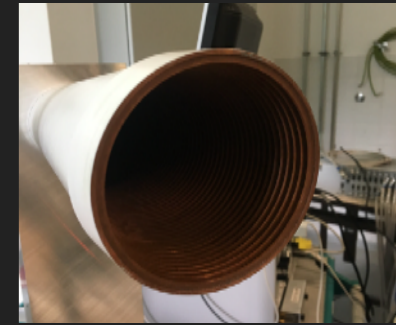


Correlation length 35 mm

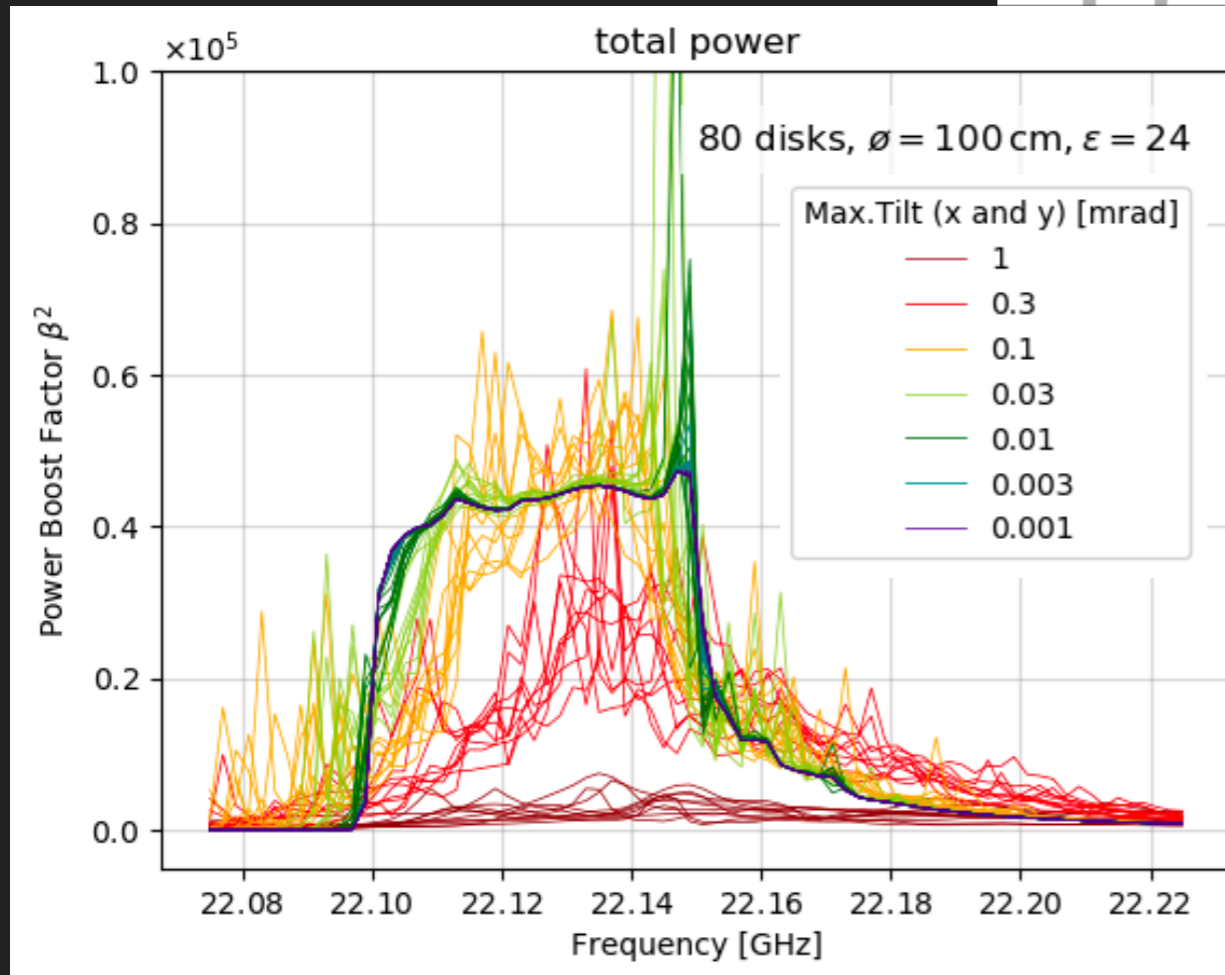
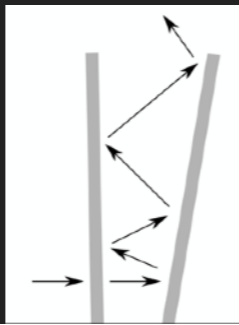


- Disc flatness better than 5 μm is desirable; 10 μm is critical
- Effects on boost factor may be mitigated through measurement-based tuning

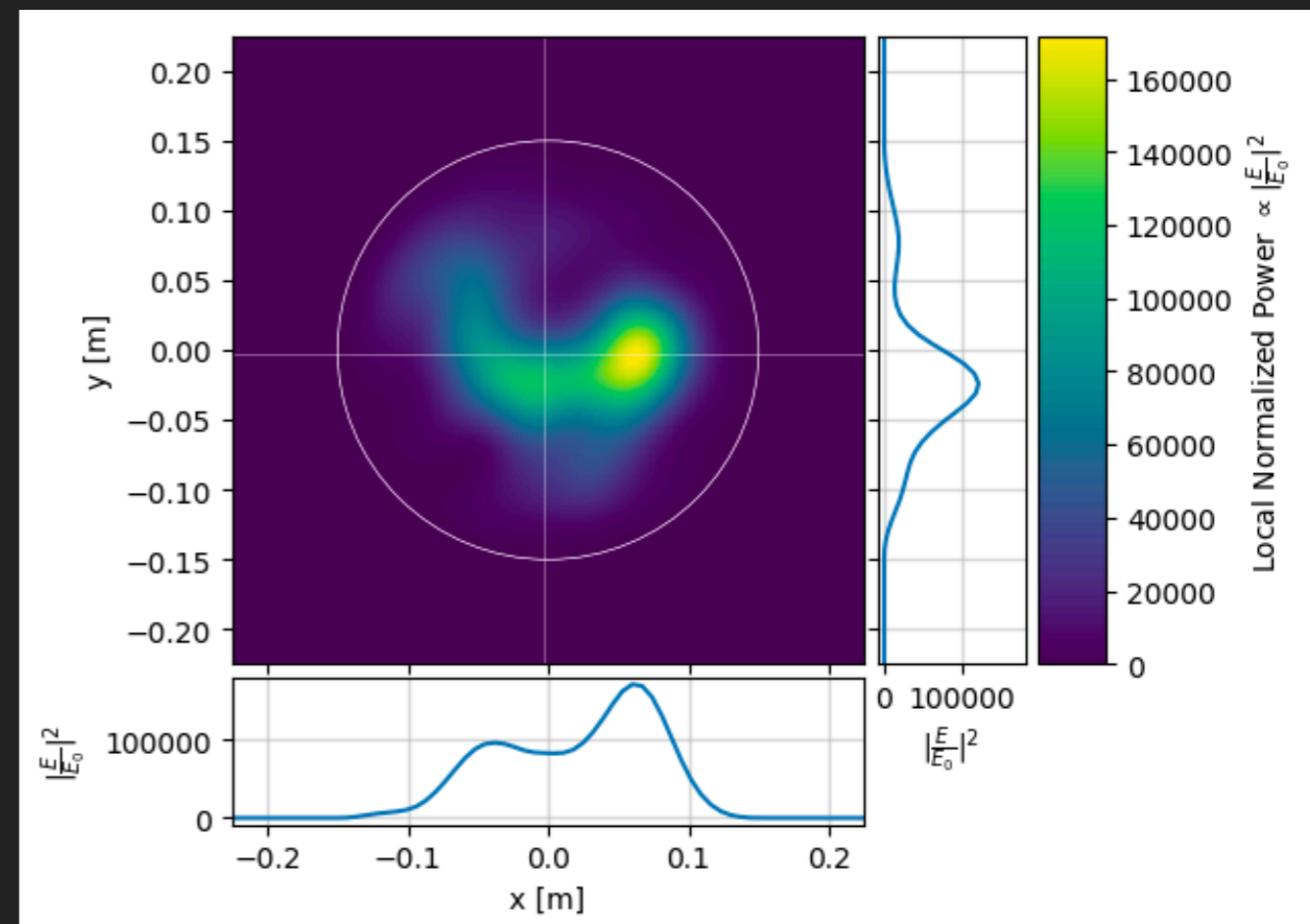
CRITICAL DESIGN PARAMETERS (3)



▶ Disc tilting



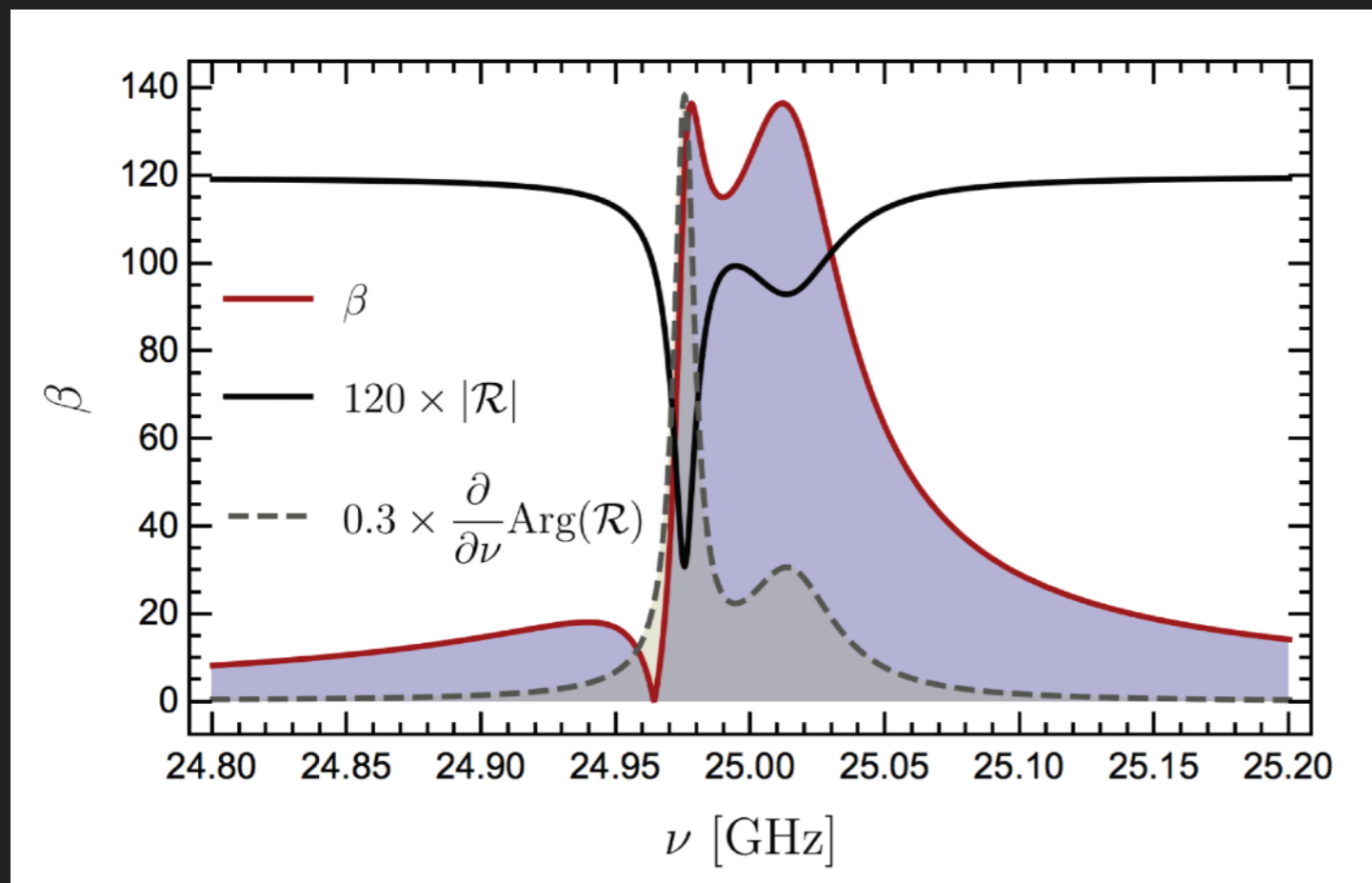
- ▶ Non-ideal discs result in irregular beam shapes
 - ▶ How to efficiently couple such a beam into the receiver is under study



- ▶ For 1-m discs, disc tilting should be less than 0.1 mrad (100 μ m)

FREQUENCY TUNING

- ▶ Boost factor cannot be measured experimentally
- ▶ It can be inferred from measurements of the electromagnetic response such as the reflectivity, as it is strongly correlated with the boost factor

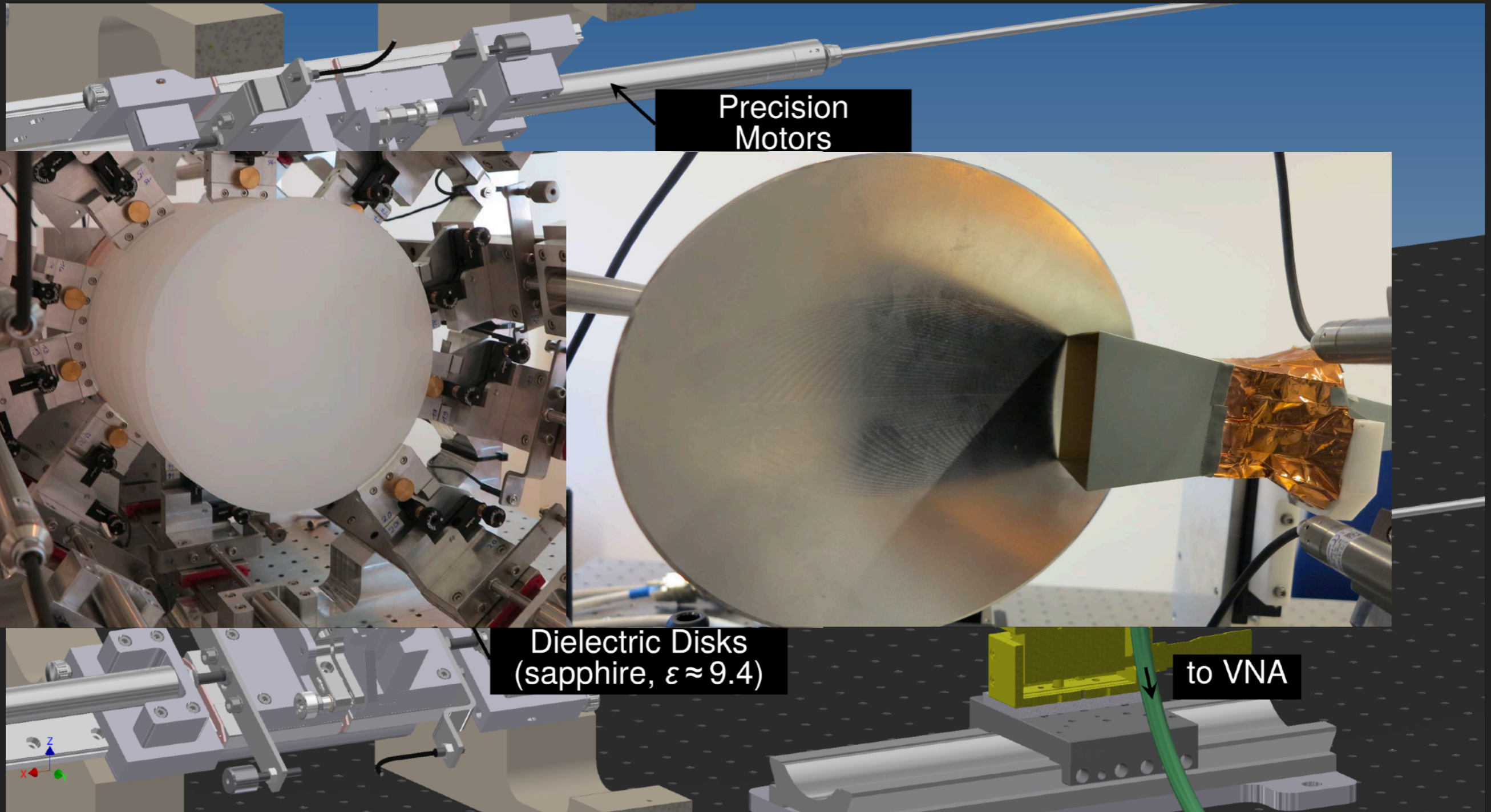


20 discs, 1 mm-thick, $\epsilon = 25$

- ▶ **Group delay** $\frac{\partial}{\partial \nu} \arg(\mathcal{R})$ maps out the resonances within the booster
 - ▶ Near frequencies that experience a large number of internal reflections, the phase of the reflected radiation changes rapidly.

PROOF-OF-PRINCIPLE SETUP

J. Egge, S. Knirck, et. al. [arXiv:2001.04363](https://arxiv.org/abs/2001.04363)



ANTENNA EFFECTS

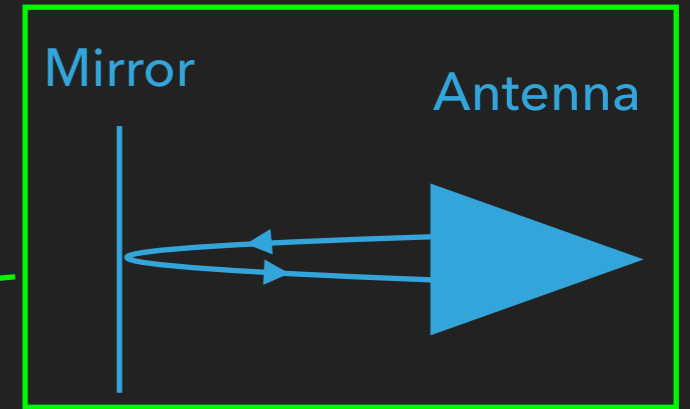
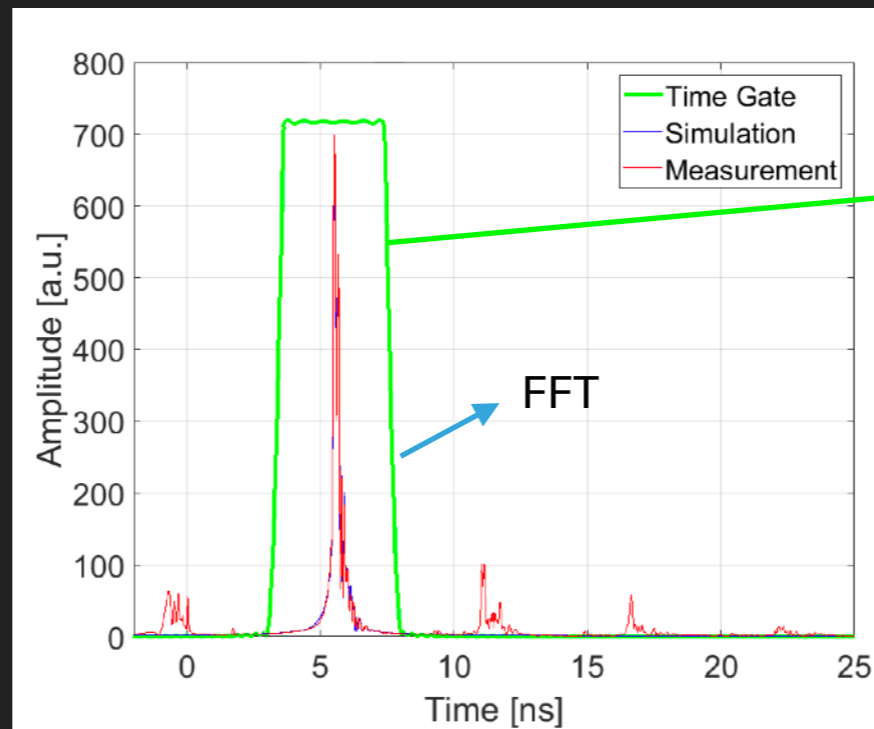
- ▶ Antenna-mirror efficiency

Assumption: adding discs does not significantly alter the beam shape

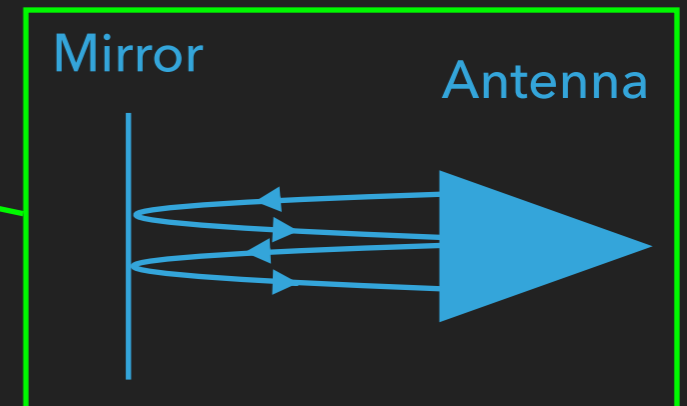
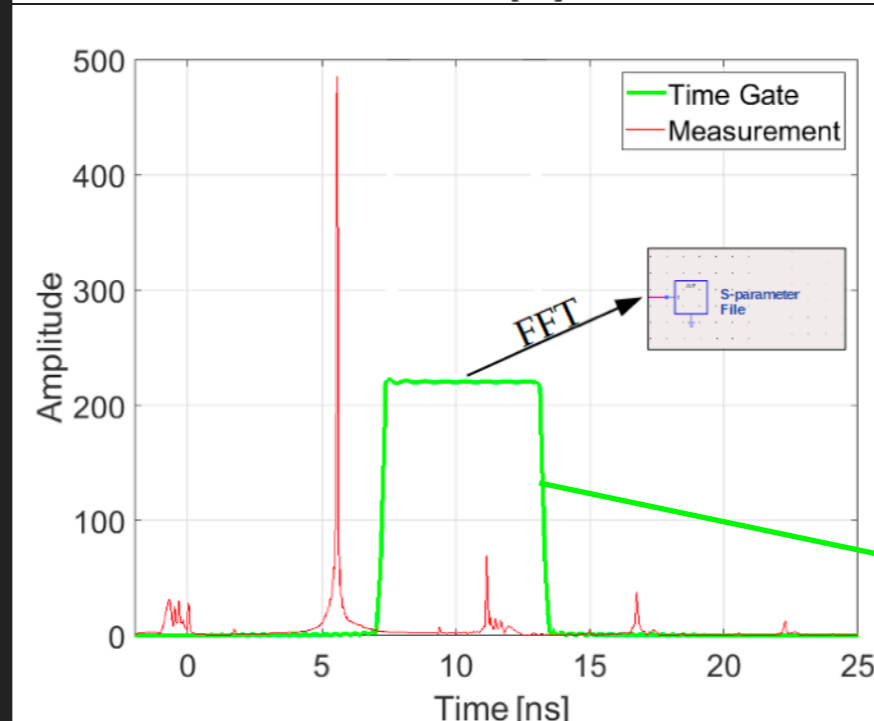
- ▶ Impedance mismatch between the antenna and free space

- ▶ Included in simulation

Reflectivity of the antenna-mirror system in time domain

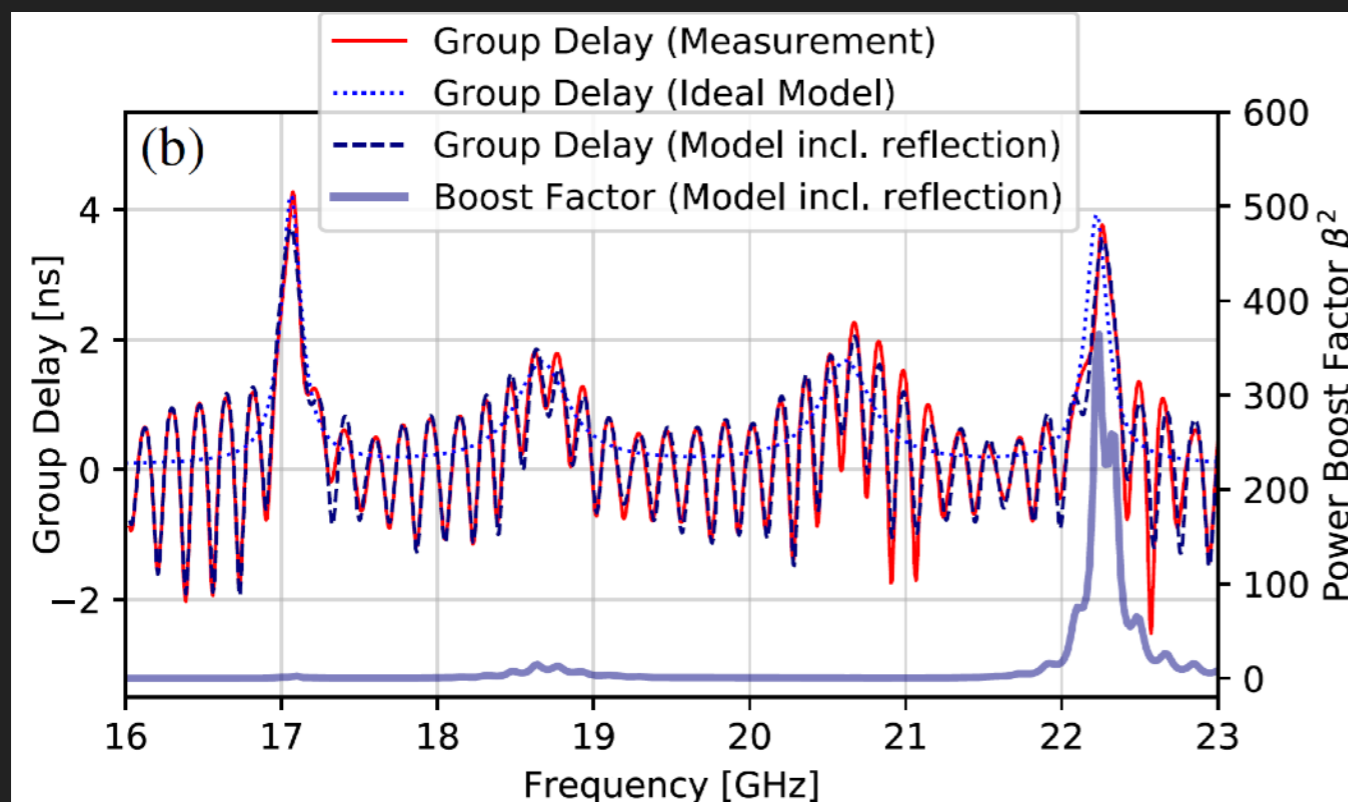


More sophisticated antenna model is needed



REFLECTIVITY MEASUREMENT AND FREQUENCY TUNING

Proof-of-principle setup with 4 discs

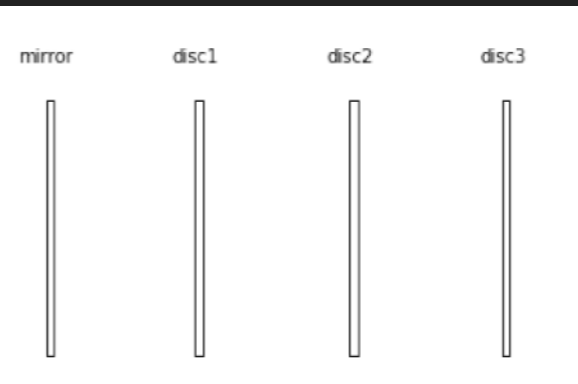
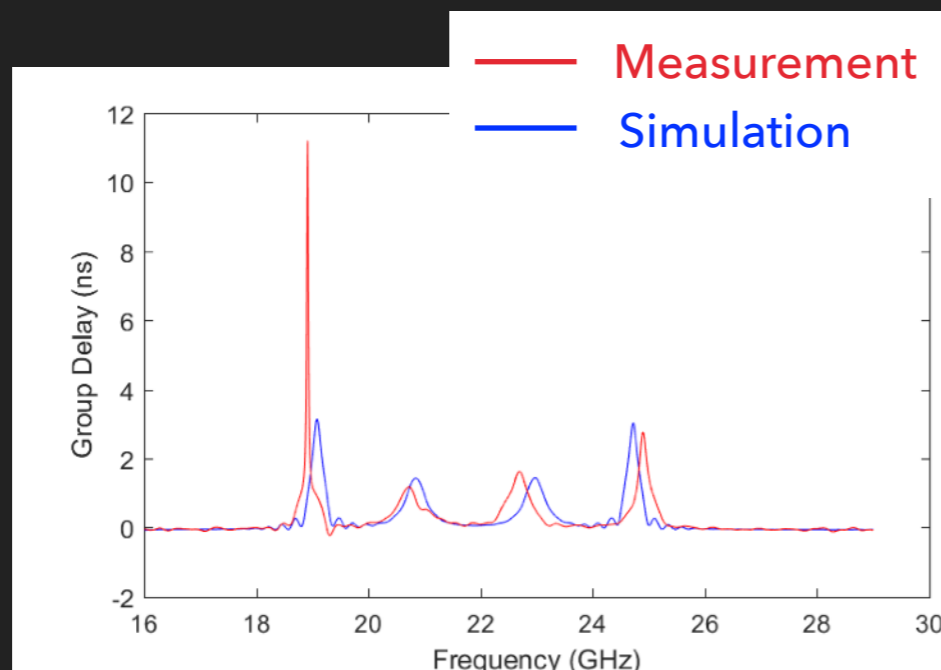


- ▶ 1D model is used
- ▶ Ripples due to the impedance mismatch at antenna aperture

- ▶ Challenges for frequency tuning
 - ▶ Absolute disc positions are not known
 - ▶ Key booster parameters such as the dielectric constant are difficult to measure precisely
 - ▶ Perfect simulation does not exist
- ▶ These issues can be mitigated by a **measurement-based tuning procedure**

DISC TUNING PROCEDURE

1. Adjust the disc spacings in the simulation to obtain the desired boost factor
 - ▶ Calculate the reflectivity, in particular the group delay, with the same configuration with calibrated antenna reflections included
2. Adjust the disc positions in the setup until the measured group delay matches that given by the simulation

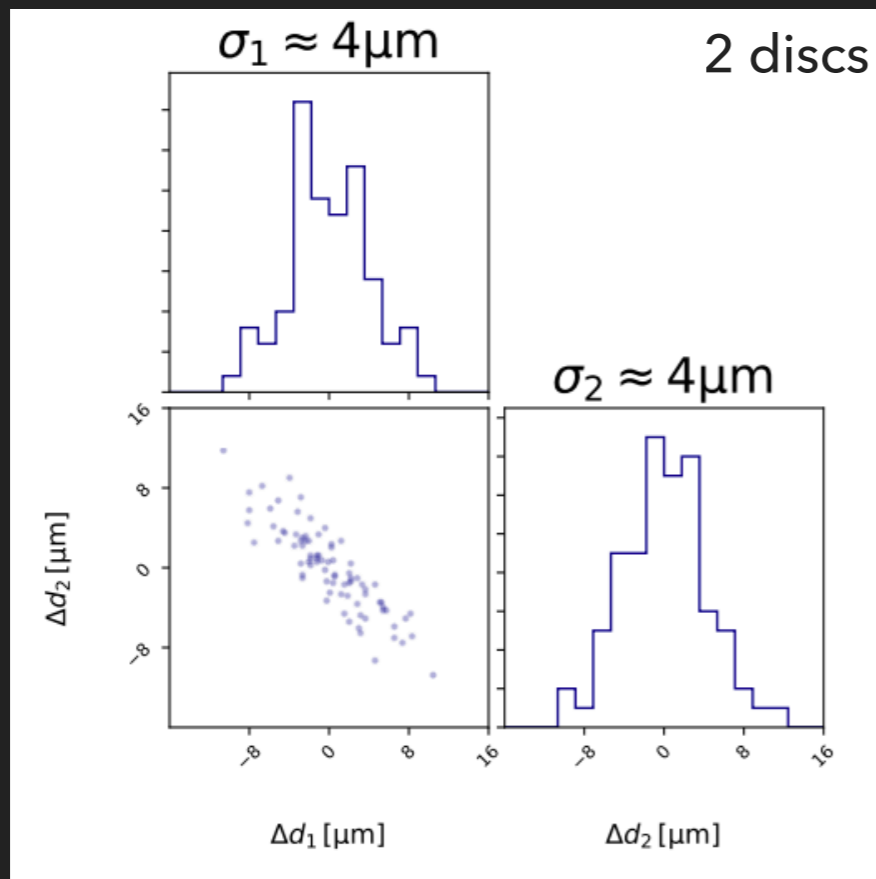


The movement is guided by an algorithm

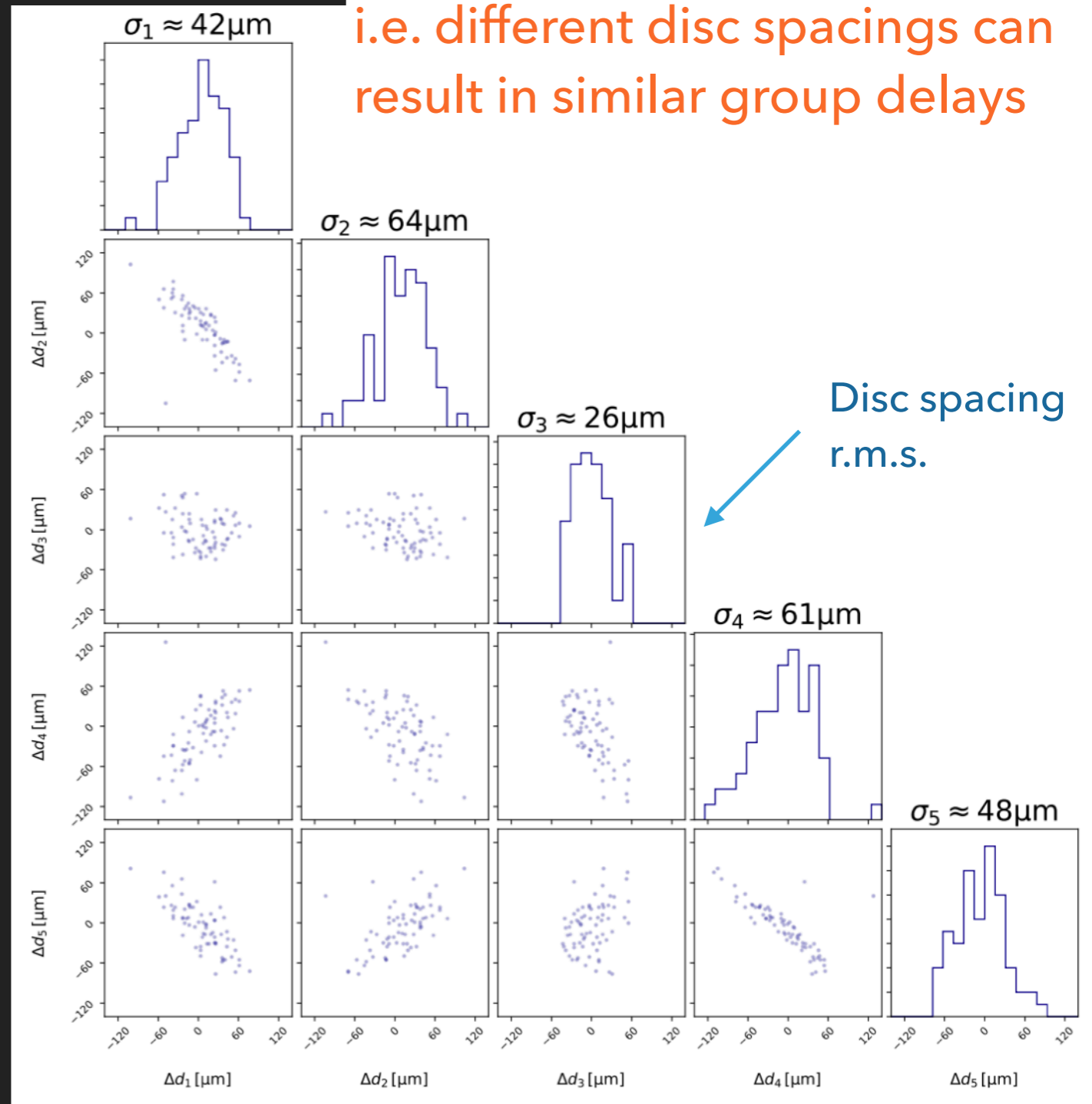
Move discs in the setup

DISC TUNING RESULTS

- ▶ In order to quantify the disc spacing repeatability, repeat step 2 with different random starting positions ~200 times

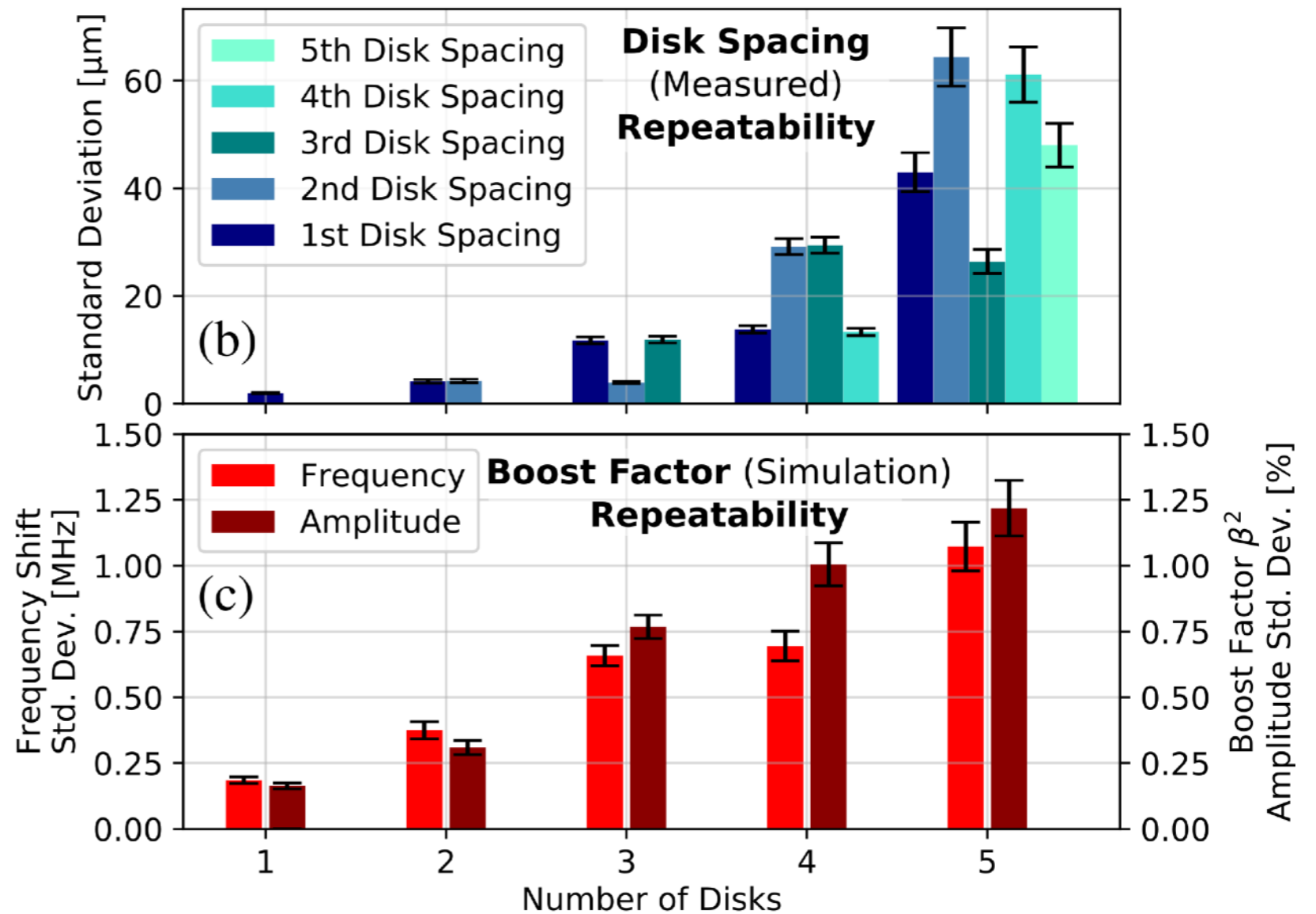
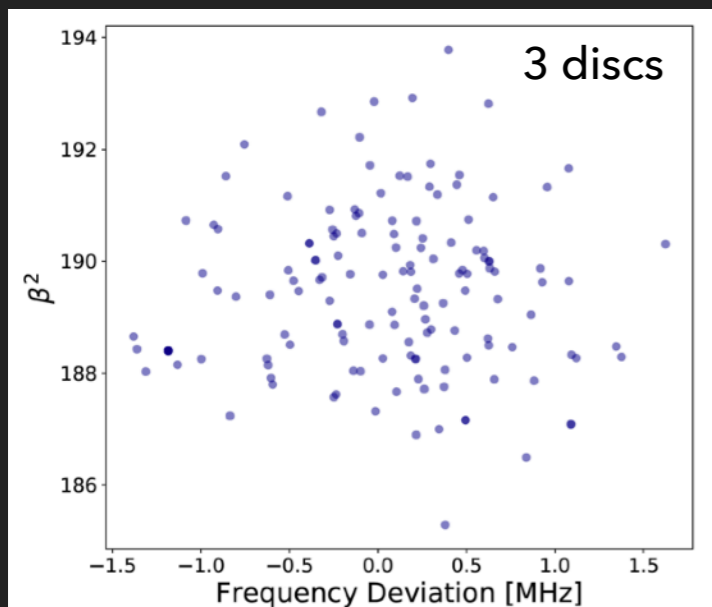


5 discs



UNCERTAINTY OF THE BOOST FACTOR DUE TO TUNING

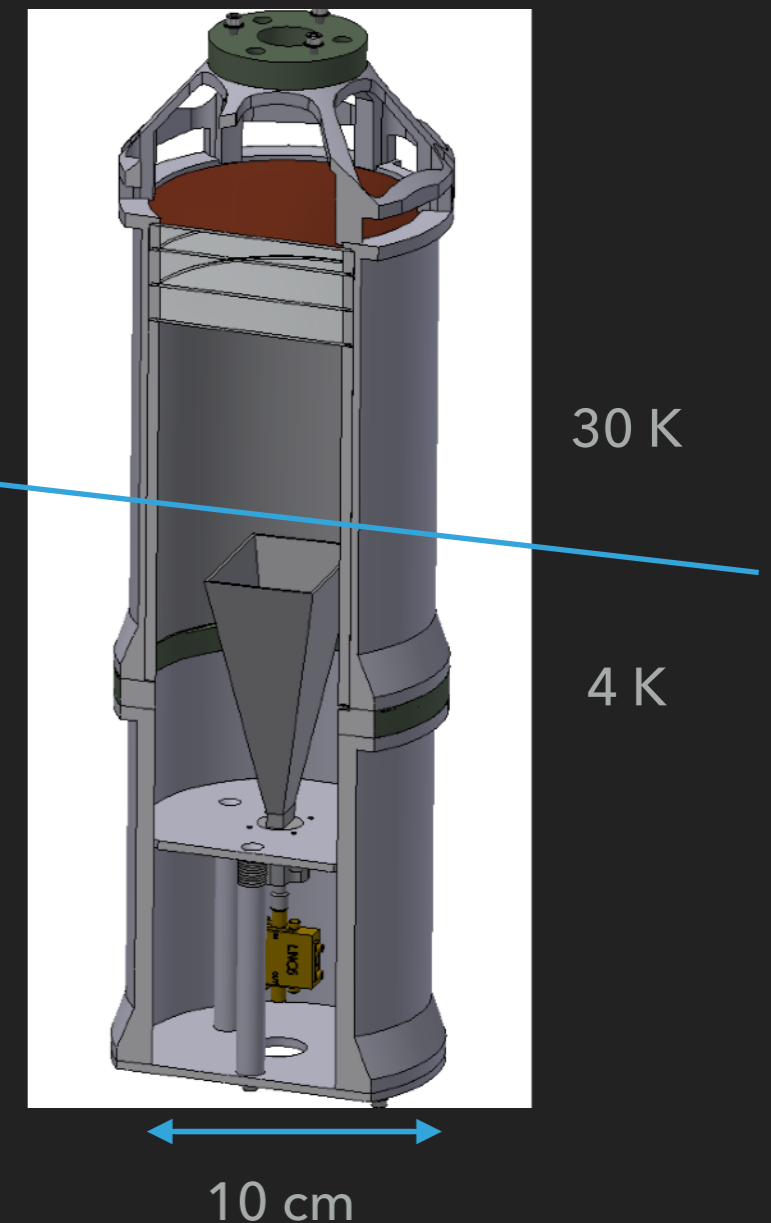
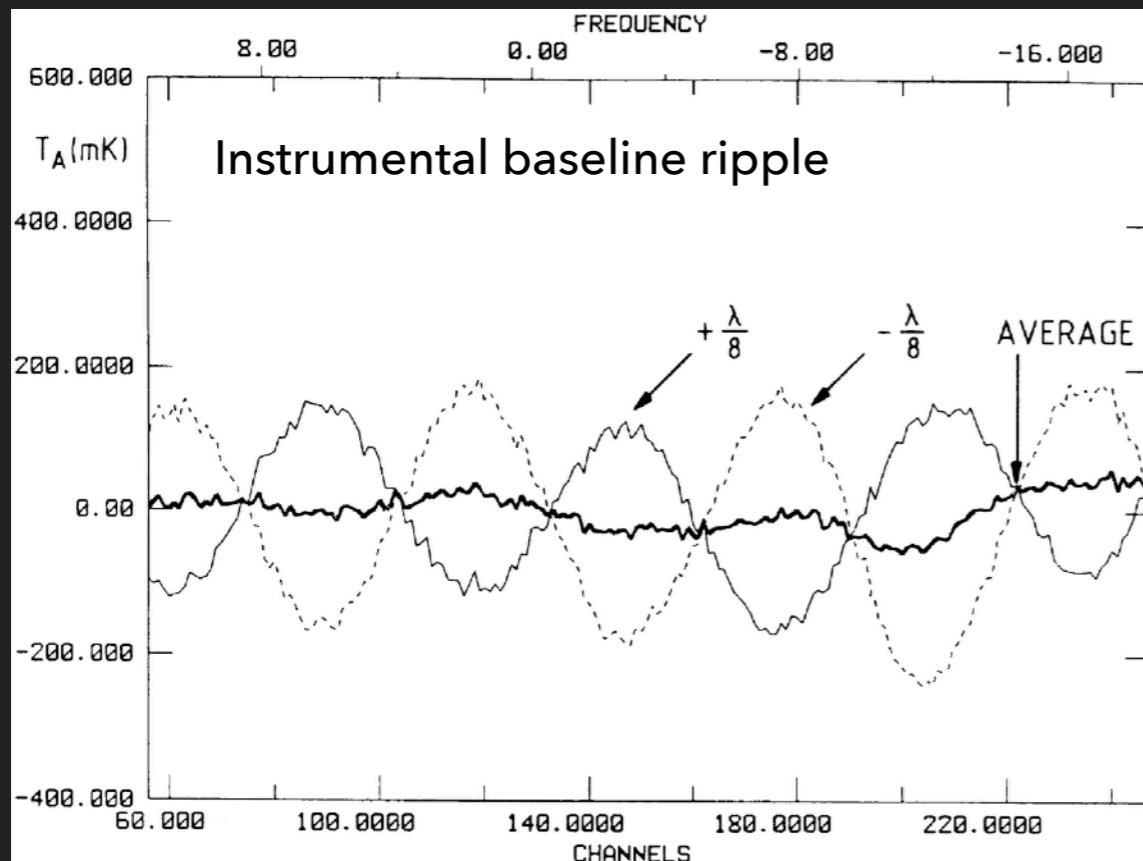
- ▶ Degenerate disc spacings → uncertainties on the boost factor



SYSTEM NOISE TEMPERATURE

- ▶ $SNR = \frac{P_{sig}}{k_B T_{sys}} \sqrt{\frac{t_{scan}}{\Delta\nu}}$, where $T_{sys} = T_{rec} + T_{booster}$
- ▶ T_{rec} depends on receiver noise temperature and frequency

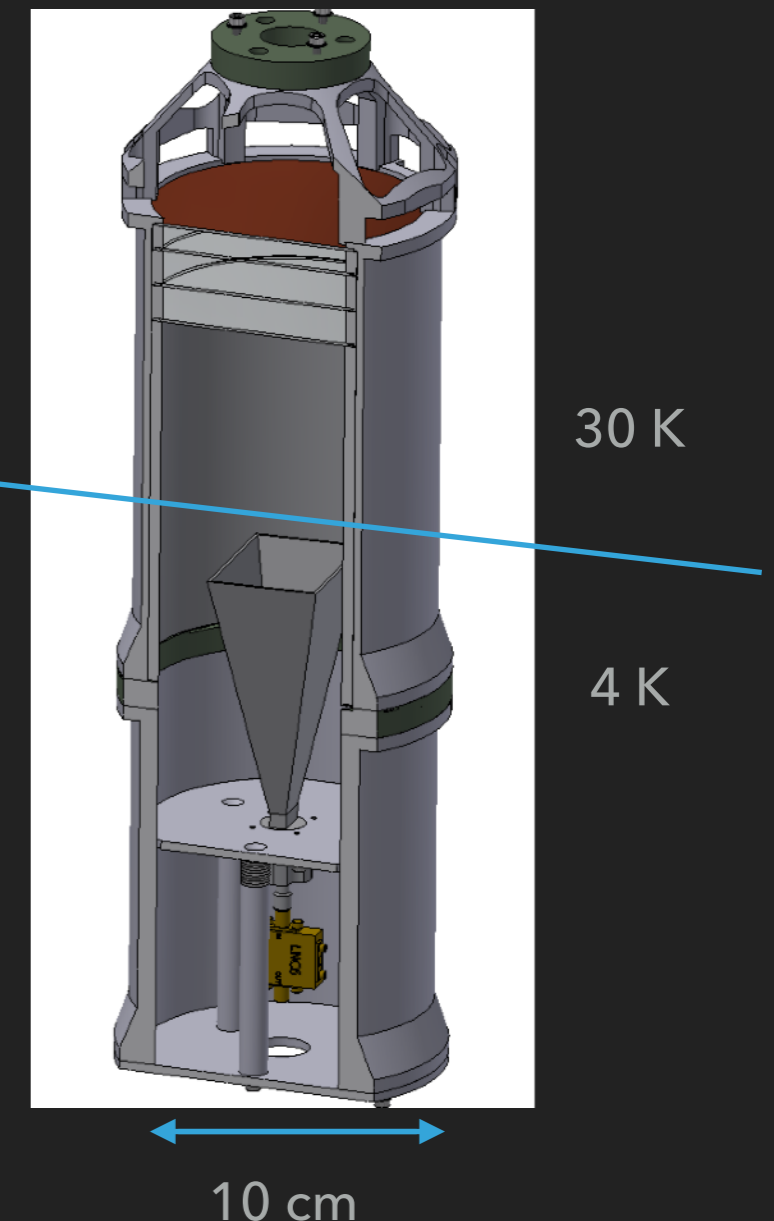
Cold measurement of system noise temperature ongoing



SYSTEM NOISE TEMPERATURE

- ▶ $SNR = \frac{P_{sig}}{k_B T_{sys}} \sqrt{\frac{t_{scan}}{\Delta\nu}}$, where $T_{sys} = T_{rec} + T_{booster}$
- ▶ T_{rec} depends on receiver noise temperature and frequency
- ▶ Kirchhoff theorem: $T_{booster} = \epsilon \cdot T_{physical}$
 - ▶ Emissivity $\epsilon = 0$ for perfect electrical conductor, $\epsilon = 1$ for perfect blackbody
 - ▶ ϵ can be reduced by choosing low $\tan \delta$ loss material for the discs and low loss metal for the mirror
 - ▶ Booster ϵ has frequency dependence

Cold measurement of system noise temperature ongoing



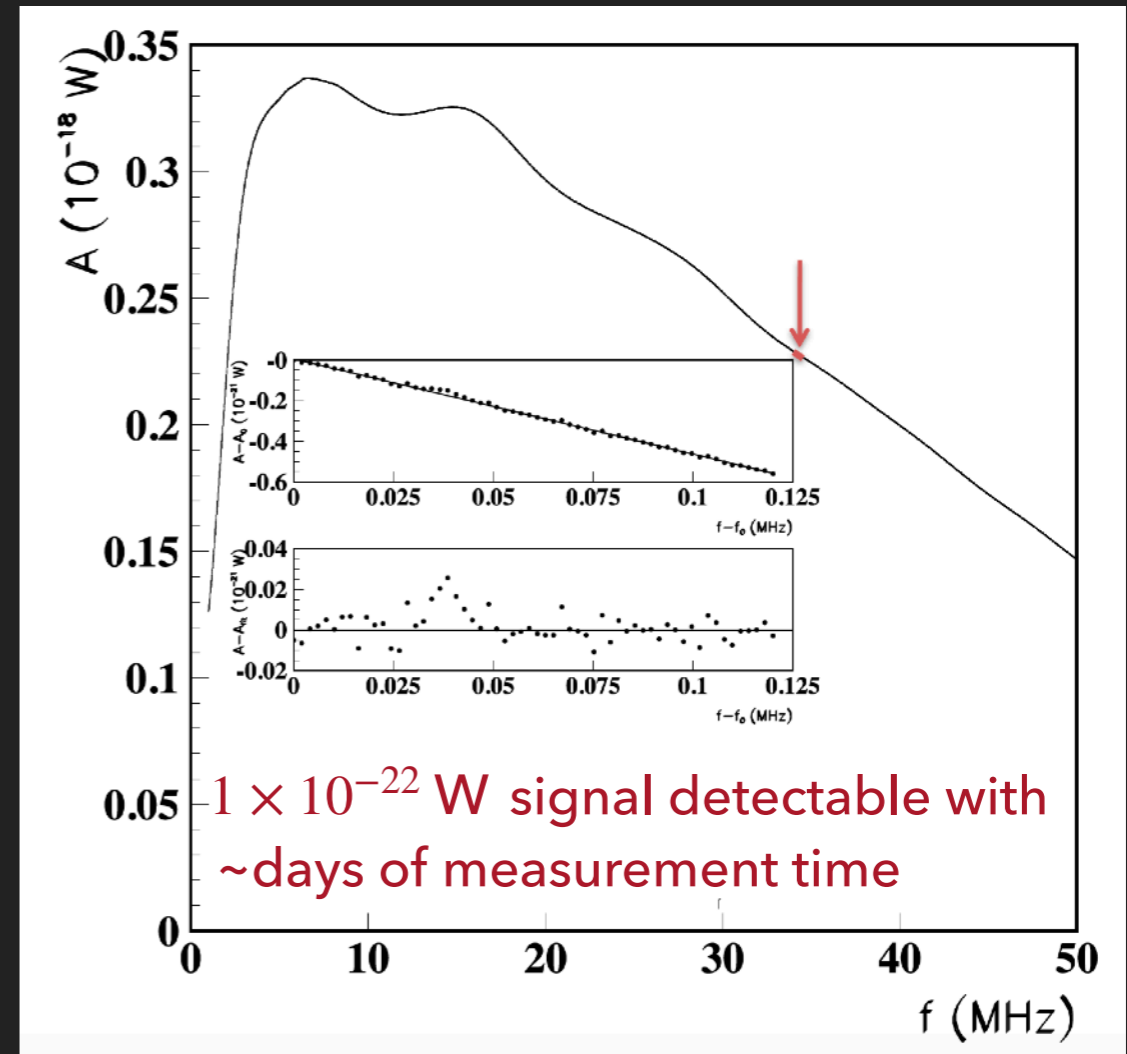
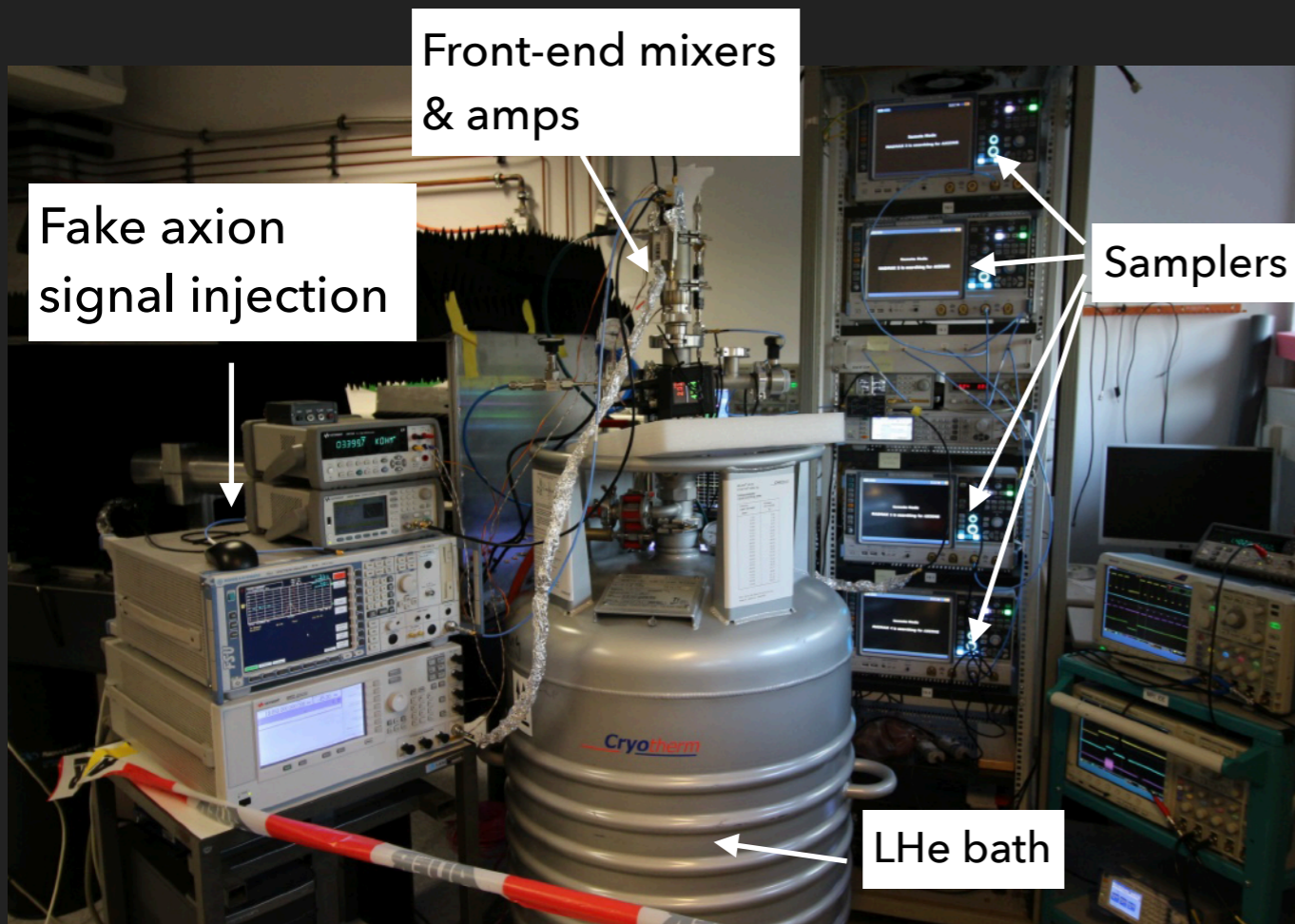
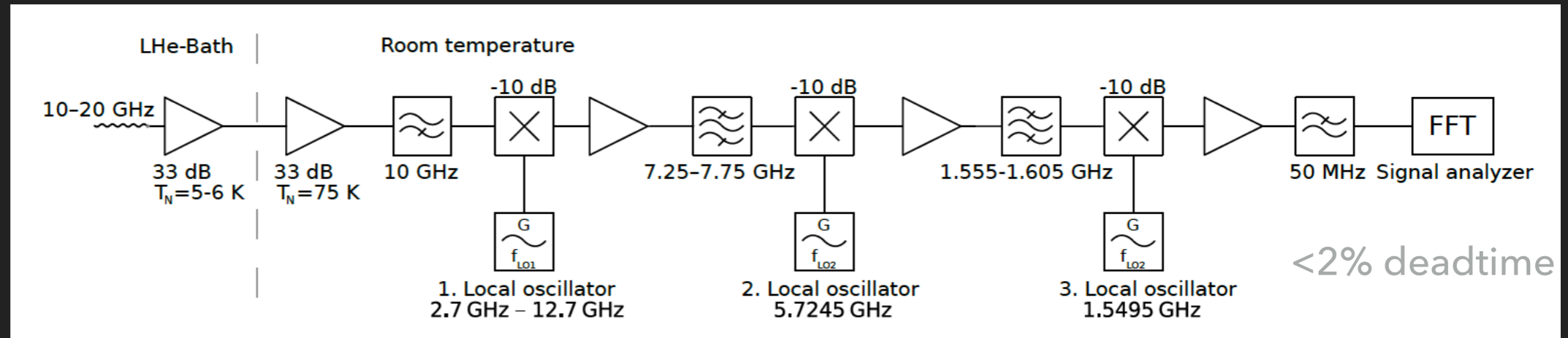
RECEIVER CHAIN

Below 40 GHz linear amplifier most suitable



HEMT amplifier from Low Noise Factory

$$T_{rec} = 5 - 6 \text{ K}$$

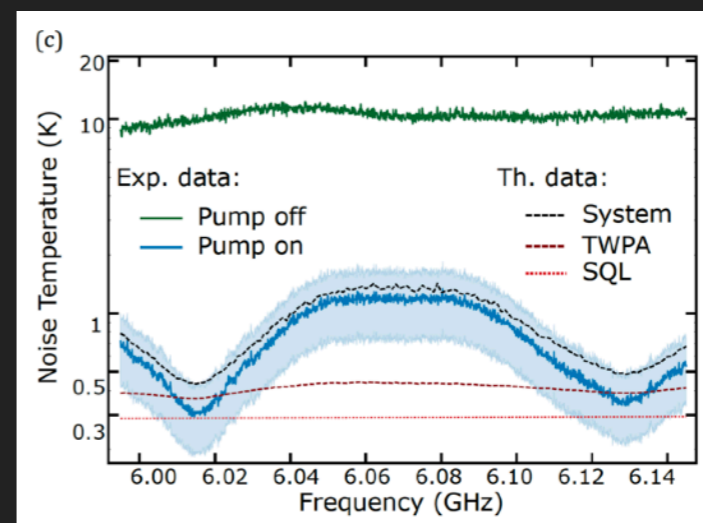
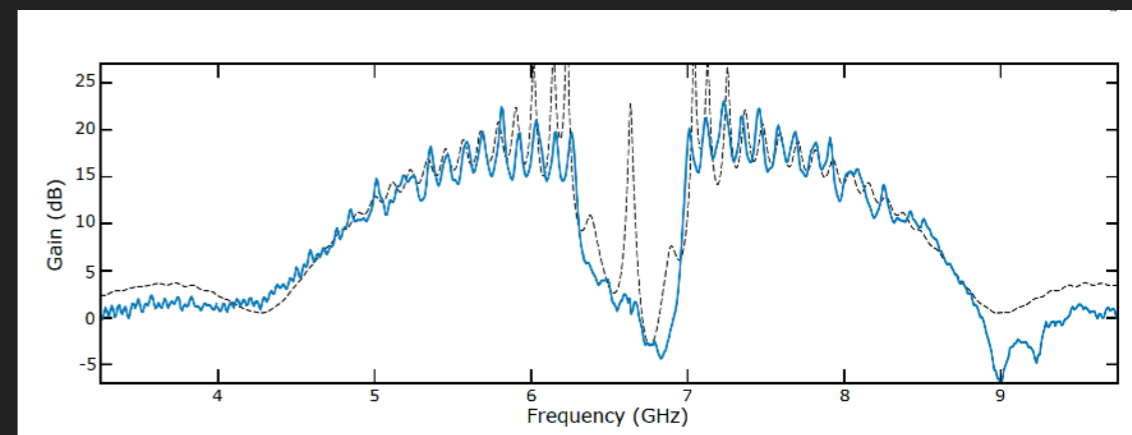
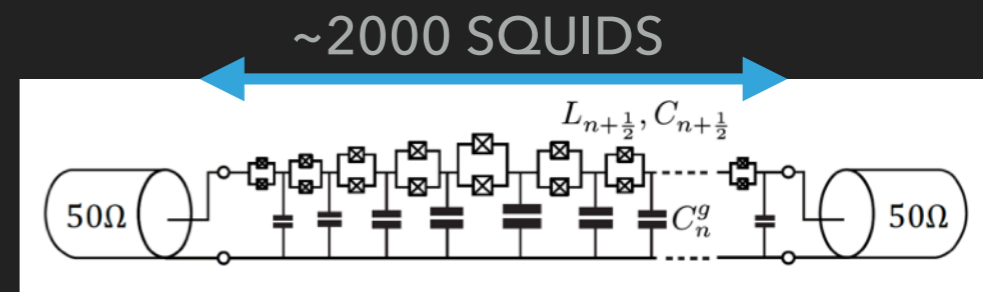


TRAVELING WAVE AMPLIFIER

- ▶ Quantum limit of coherent detectors:

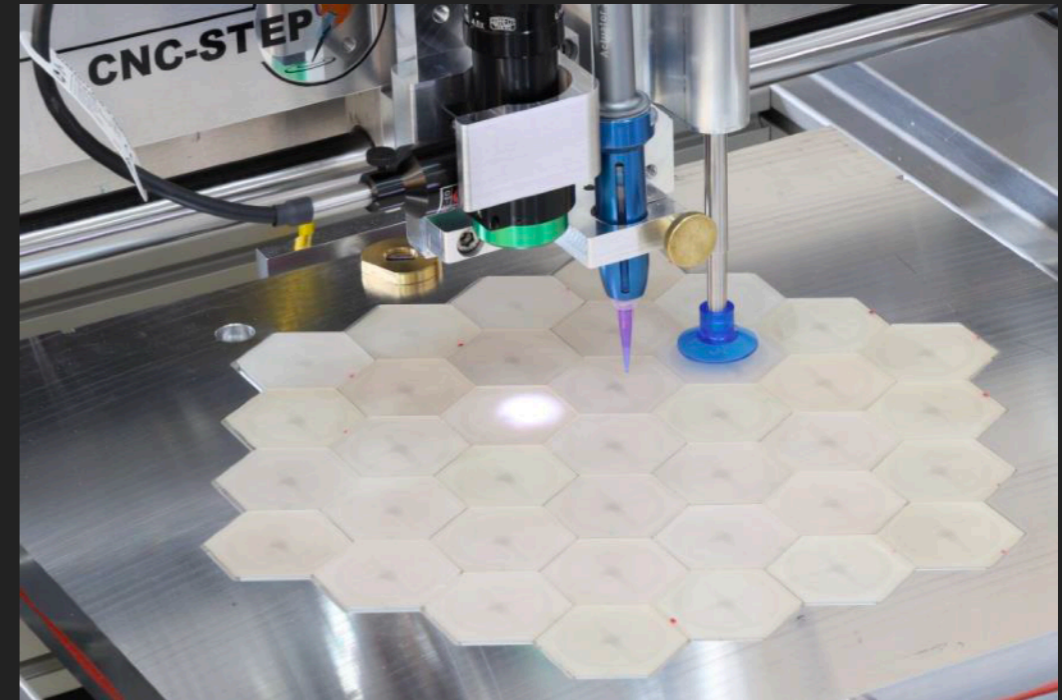
$$k_B T_{rec} = h\nu N_A, \text{ where } N_A \geq \frac{1}{2}$$

- ▶ Broadband traveling wave JPA could potentially halve system noise temperature for MADMAX
 - ▶ Josephson junction nonlinear inductance
 - ▶ GHz bandwidth
 - ▶ High 1-dB compression point
 - ▶ No need to tune frequently
 - ▶ 10-40 GHz possible with the current fabrication technology
- ▶ Testing of ~12 GHz device this summer



DIELECTRIC DISC

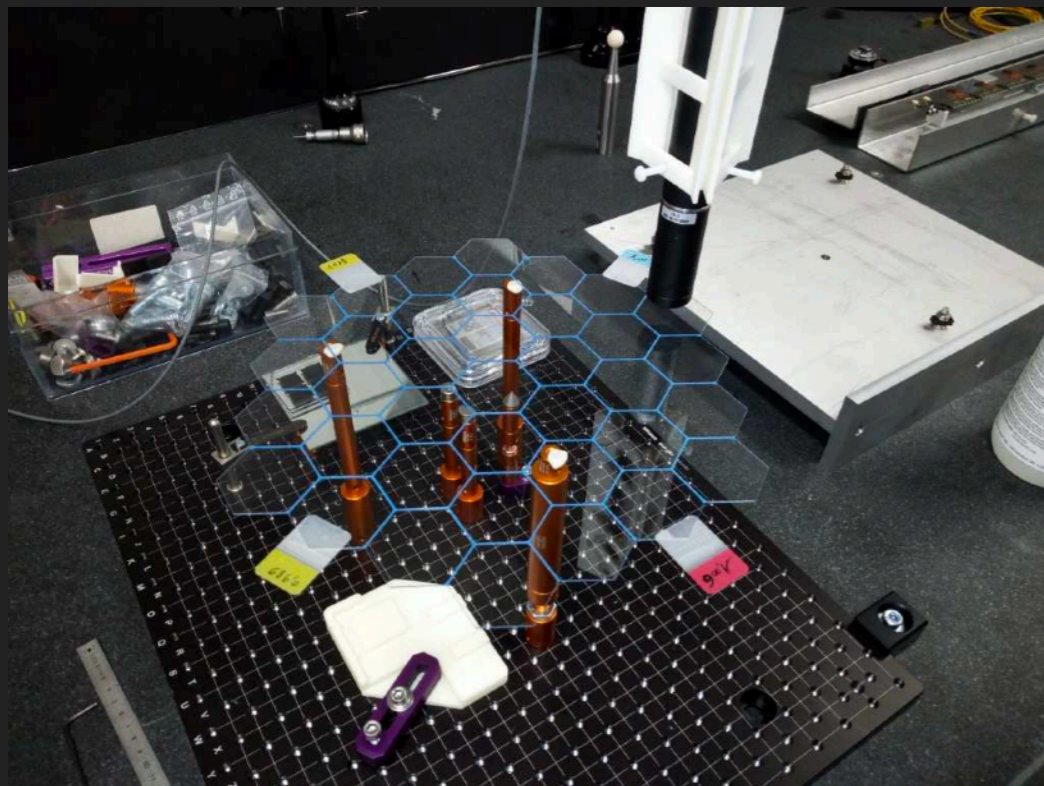
- ▶ Discs are 1.25 m in diameter and 1mm in thickness
- ▶ Candidate materials:
 - ▶ LaAlO_3
 - ▶ $\epsilon \approx 24$
 - ▶ $\tan \delta = \text{a few} \times 10^{-5}$
 - ▶ Only grown on 3" wafer; tiling needed for 1 m² discs
 - ▶ Sapphire
 - ▶ $\epsilon \approx 9$ (C-cut)
 - ▶ $\tan \delta \approx 10^{-5}$
 - ▶ Up to 20"
- ▶ Other possible candidate materials are being explored



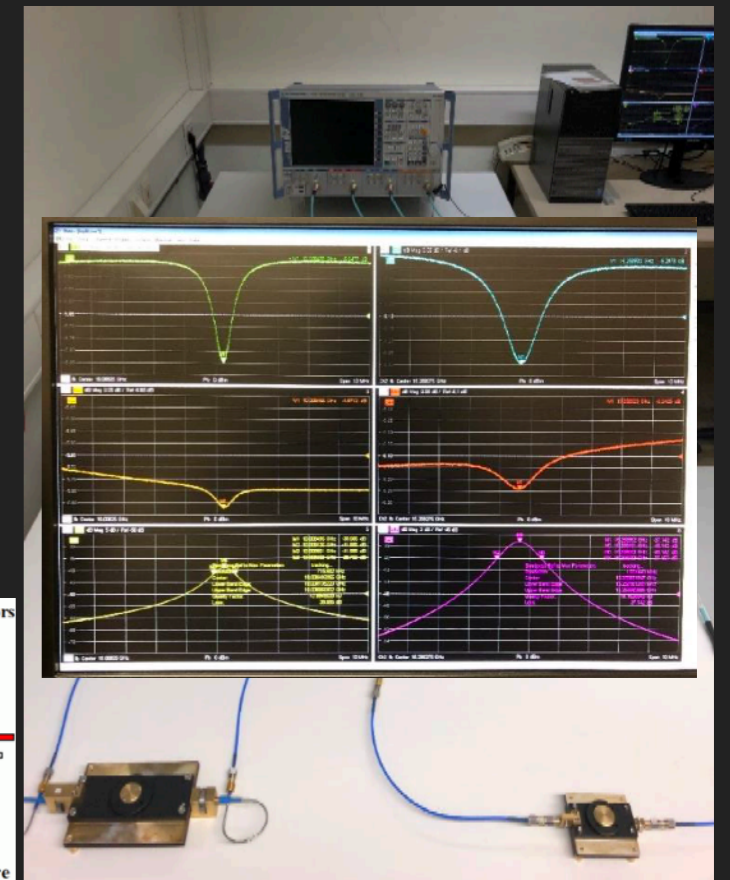
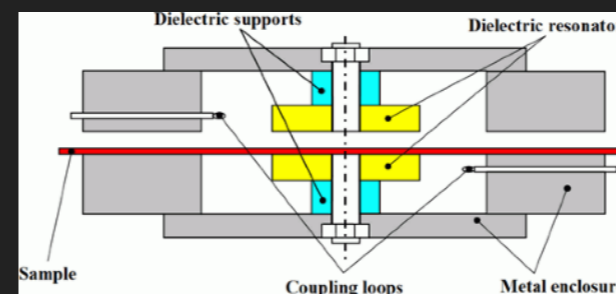
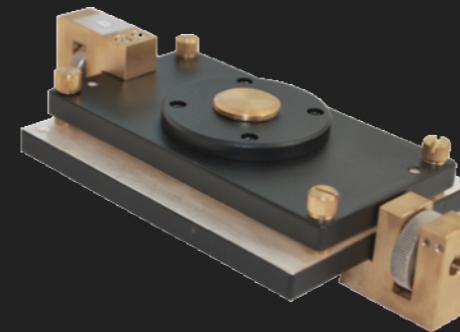
First tiled LaAlO_3 disc ($\phi = 30$ cm)

DISC CHARACTERIZATION

- ▶ Tiled disc surface is measured
 - ▶ Feedback to tiling process
- ▶ Literature values for LaAlO_3 not available at 10 to 100 GHz and/or not down to 4 K
- ▶ Highly dependent on manufacturing process

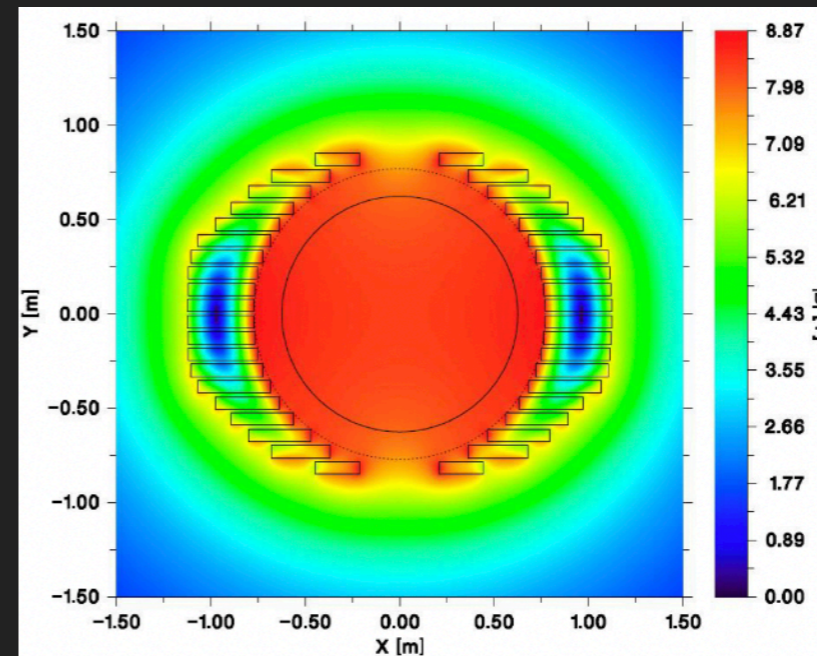
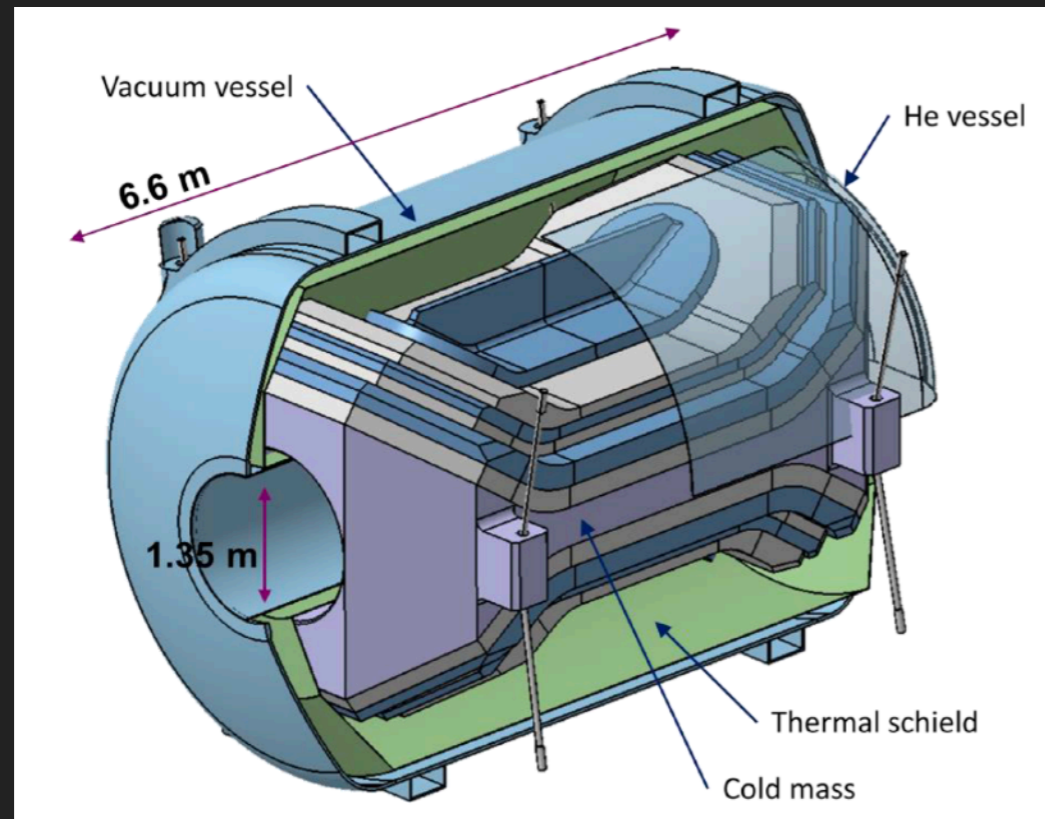


CPPM Marseille



ϵ and $\tan \delta$ measurements @ UHH

MAGNET DESIGN STUDIES



- ▶ $B^2 \cdot A \sim 100 \text{ T}^2 \text{ m}^2$ magnet has never been built before
- ▶ Working with innovation partners and an expert committee
 - ▶ NbTi coil, 9 T field, 1.25 m² aperture, ~5% inhomogeneity, 480 MJ stored energy
- ▶ Conceptual design available since 2019; the first coil may be delivered by 2021; full magnet to be commissioned by 2025

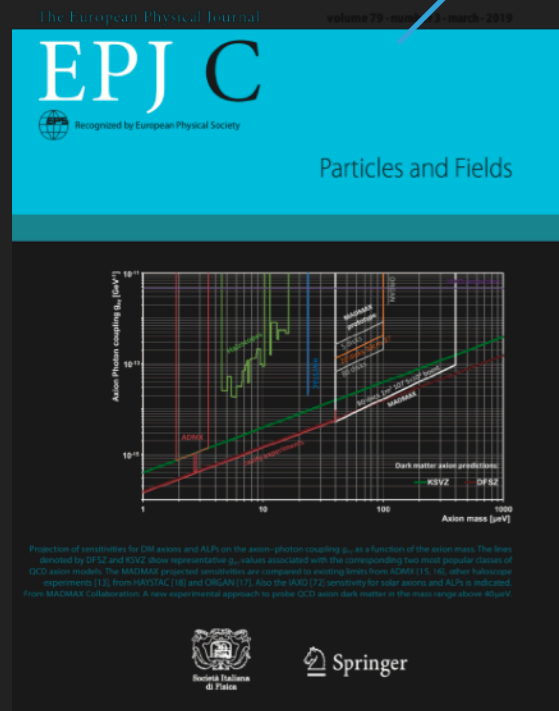
TIMELINE OF MADMAX (with abundant optimism)

2017-2019
DESIGN

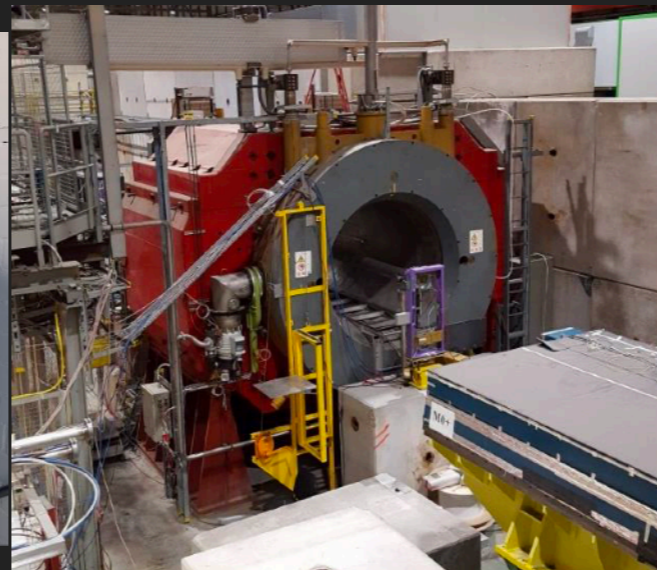
2019-2022
PROTOTYPING

2022-2025
DETECTOR CONSTRUCTION

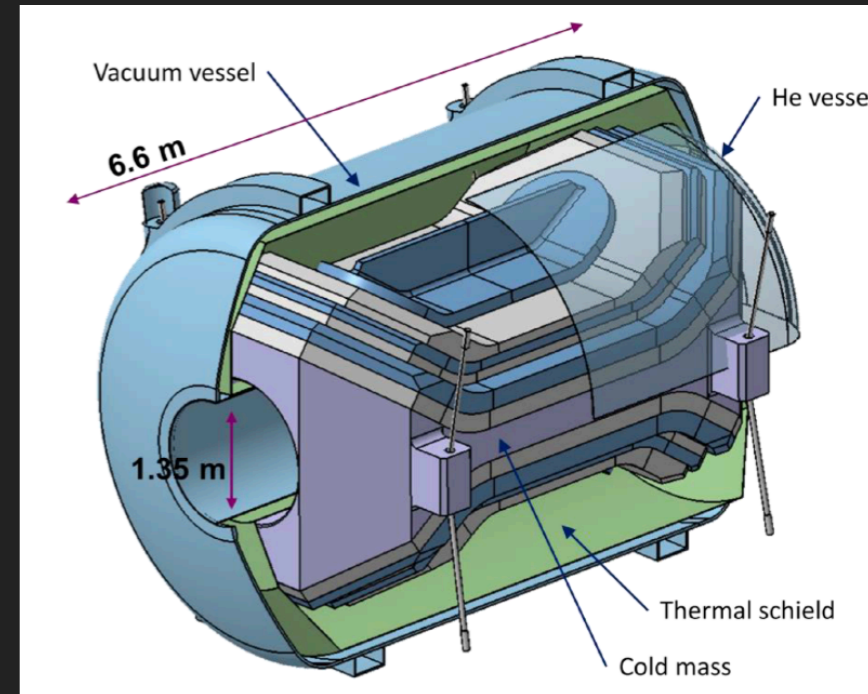
2025-2035
DATA TAKING @ DESY



RF lab SHELL @ UHH



MORPURGO magnet @ CERN up to 1.6 T



Full-size detector

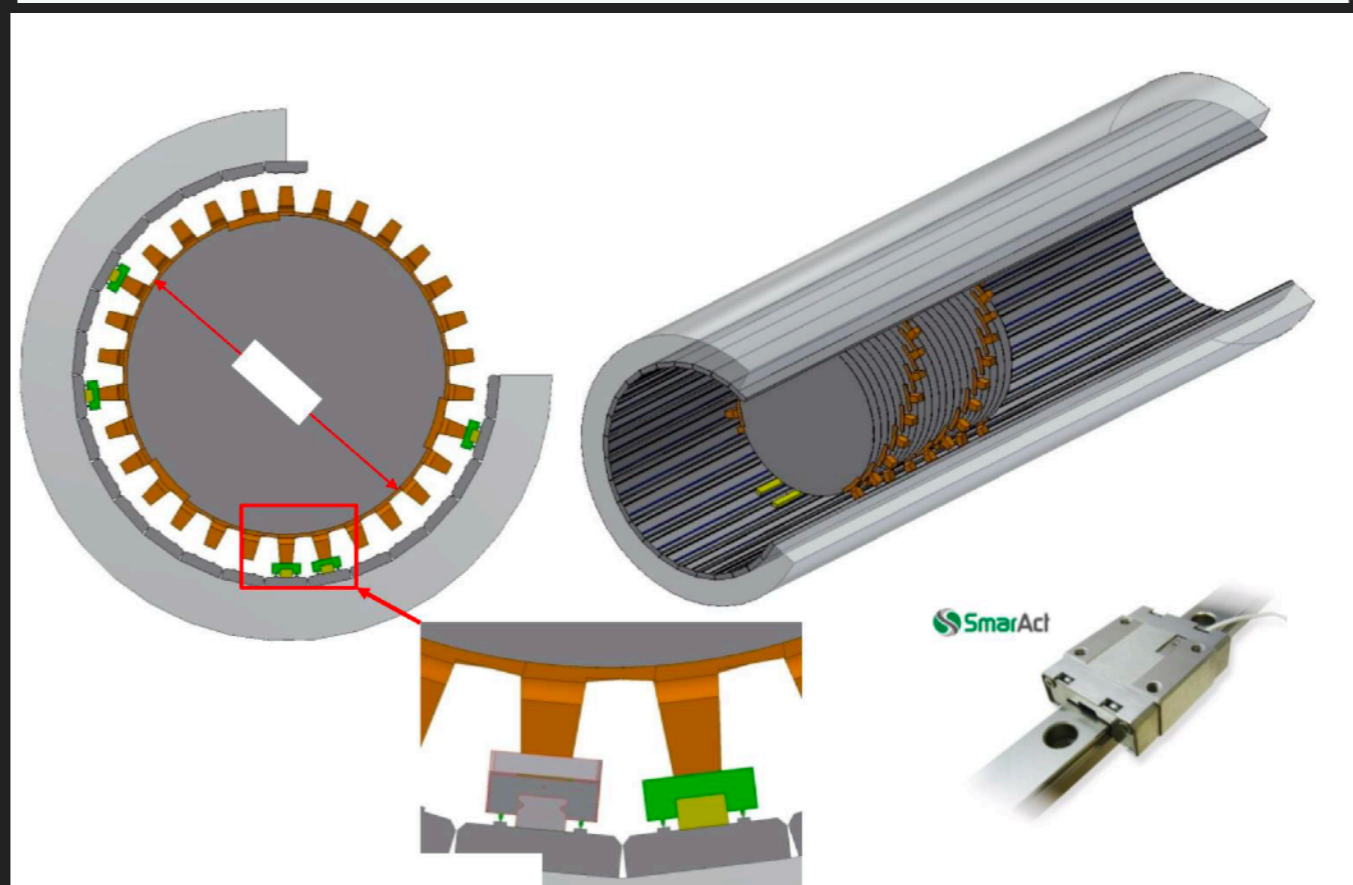
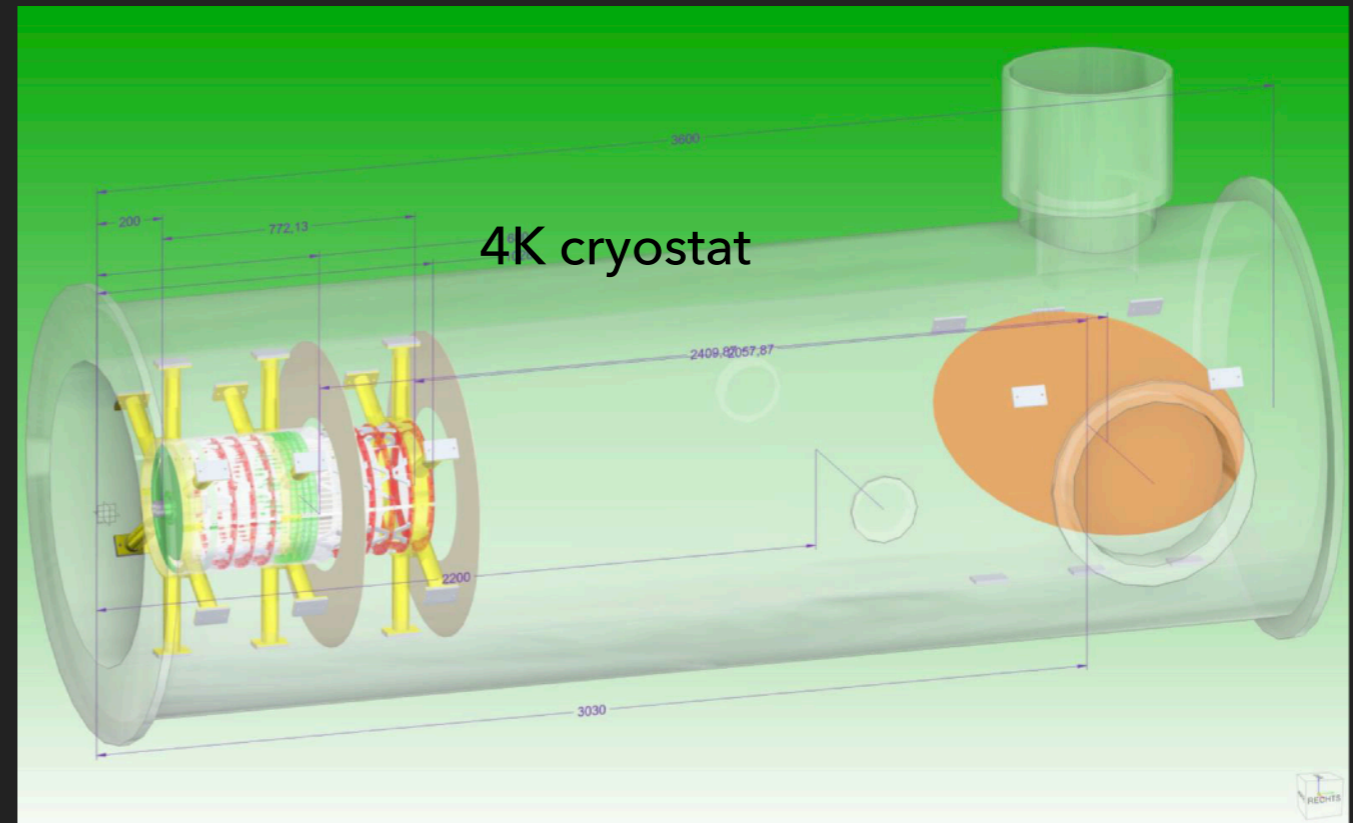
MADMAX white paper

Eur. Phys. J. C (2019) 79: 186

Prototype detector data taking

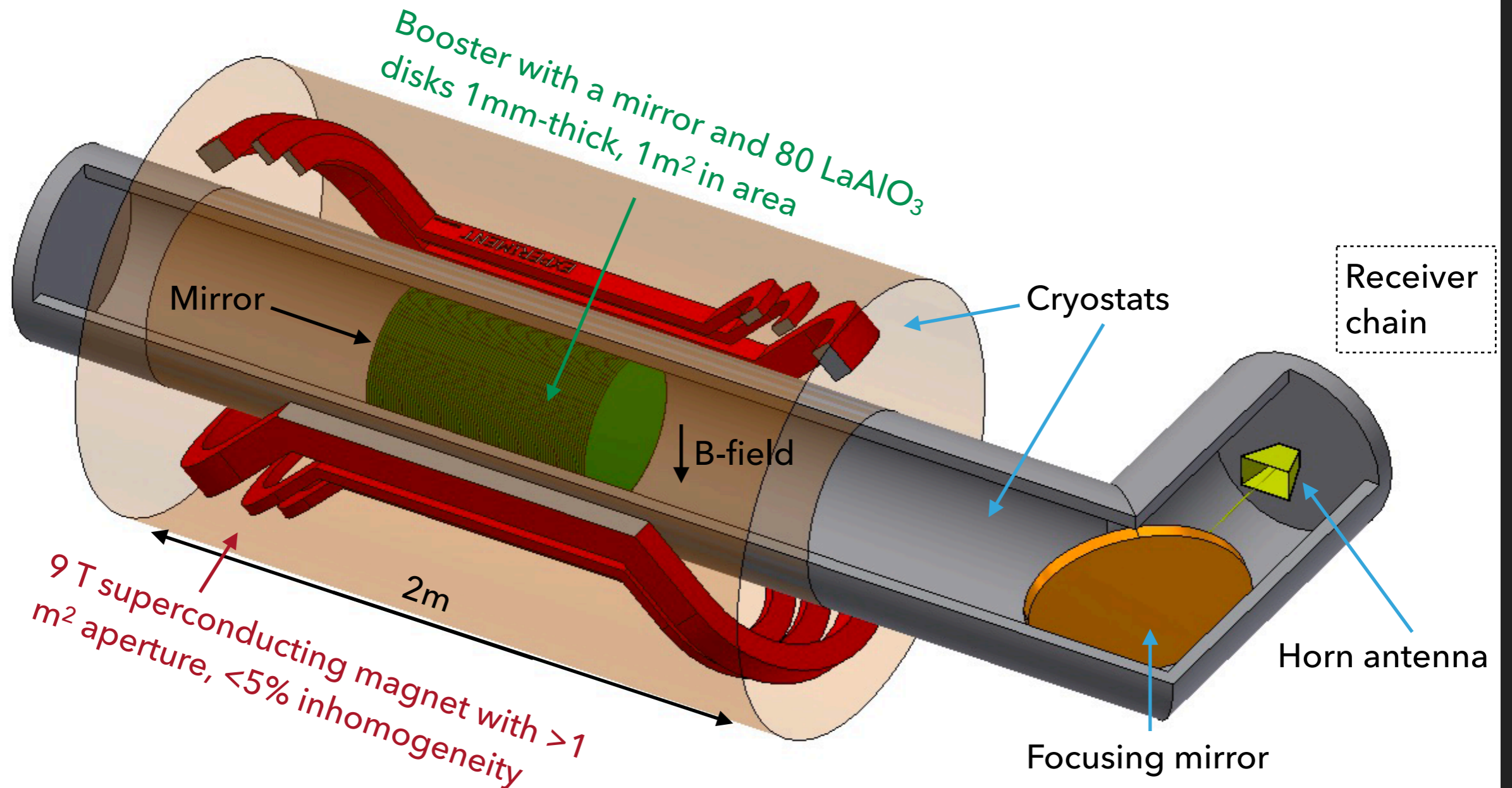
PROTOTYPE

- ▶ Aim to construct and commission prototype booster by 2022
 - ▶ 20 LaAlO_3 discs with 30cm diameter; laser interferometer incorporated
 - ▶ Hammer out the mechanical design
 - ▶ Hidden photon/ALP search
 $\sim 80 \mu\text{eV}$
- ▶ Development and testing of piezo motors are ongoing
 - ▶ 4 K, ~ 9 T, long travel range, 6 kg load bearing



MADMAX BASELINE DESIGN

Full-scale detector

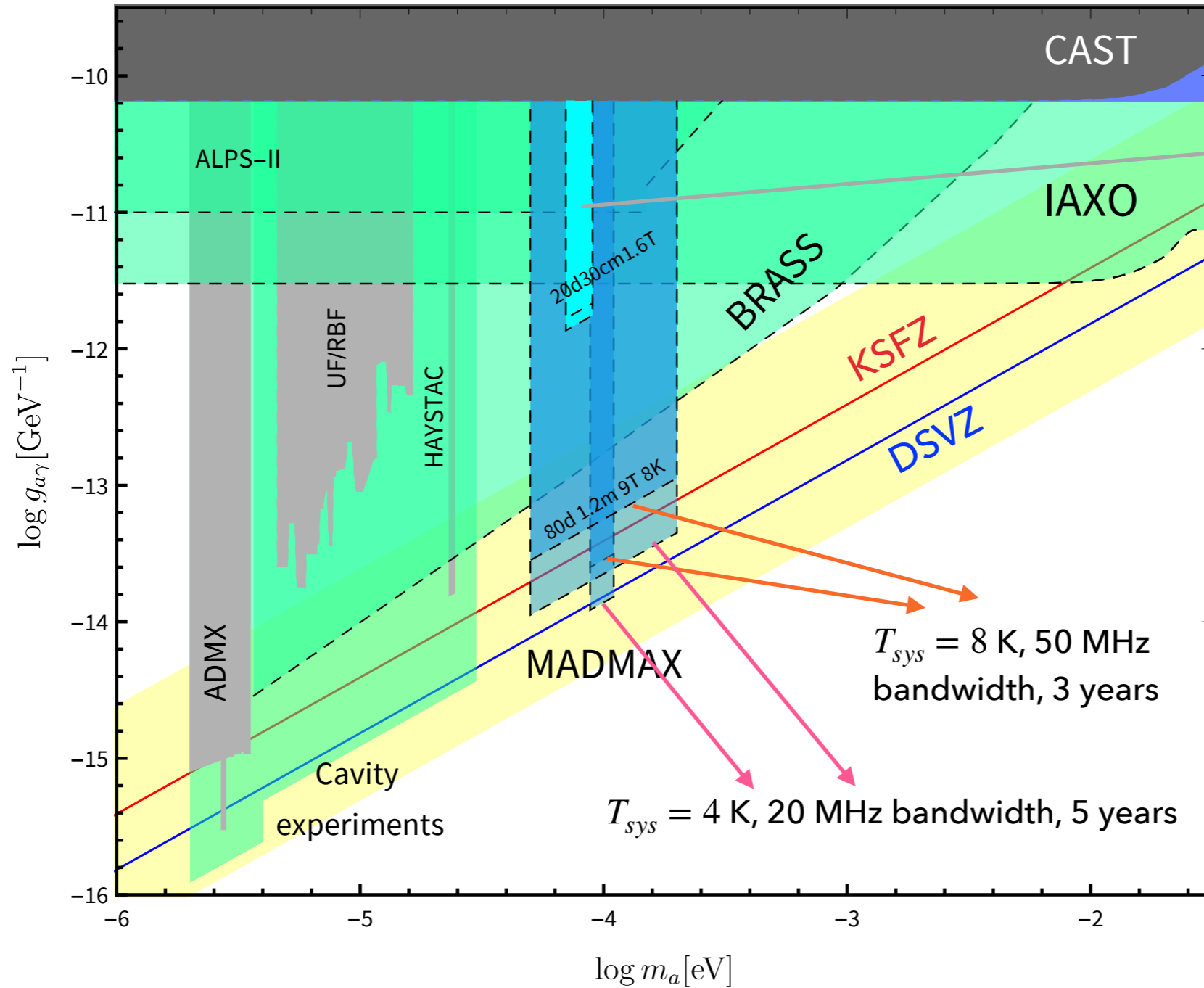


DESY SITE

- ▶ Final MADMAX detector will be located at HERA Hall North
- ▶ Make use of DESY infrastructure
- ▶ Reuse H1 yoke



MADMAX SENSITIVITY



Prototype detector
3 months

Assuming 50% of obtainable
power from 1D simulation is
received; 5σ detection level

SUMMARY AND FUTURE PROSPECT

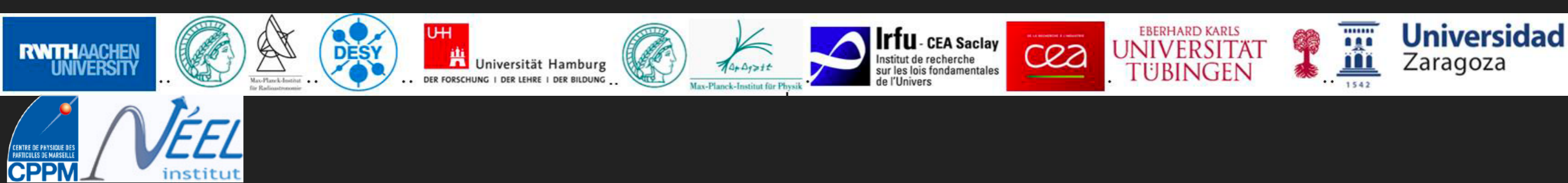
- ▶ The MADMAX experiment aims to search for QCD axions in the form of local CDM in the well-motivated mass range of $40 \sim 400 \mu\text{eV}$
 - ▶ Microwave signal at $10 \sim 100 \text{ GHz}$
 - ▶ Novel dielectric haloscope to boost axion signal to a detectable level
 - ▶ Design R&D and simulation studies are on going
 - ▶ Aim for data-taking in 2025

THE CHALLENGES

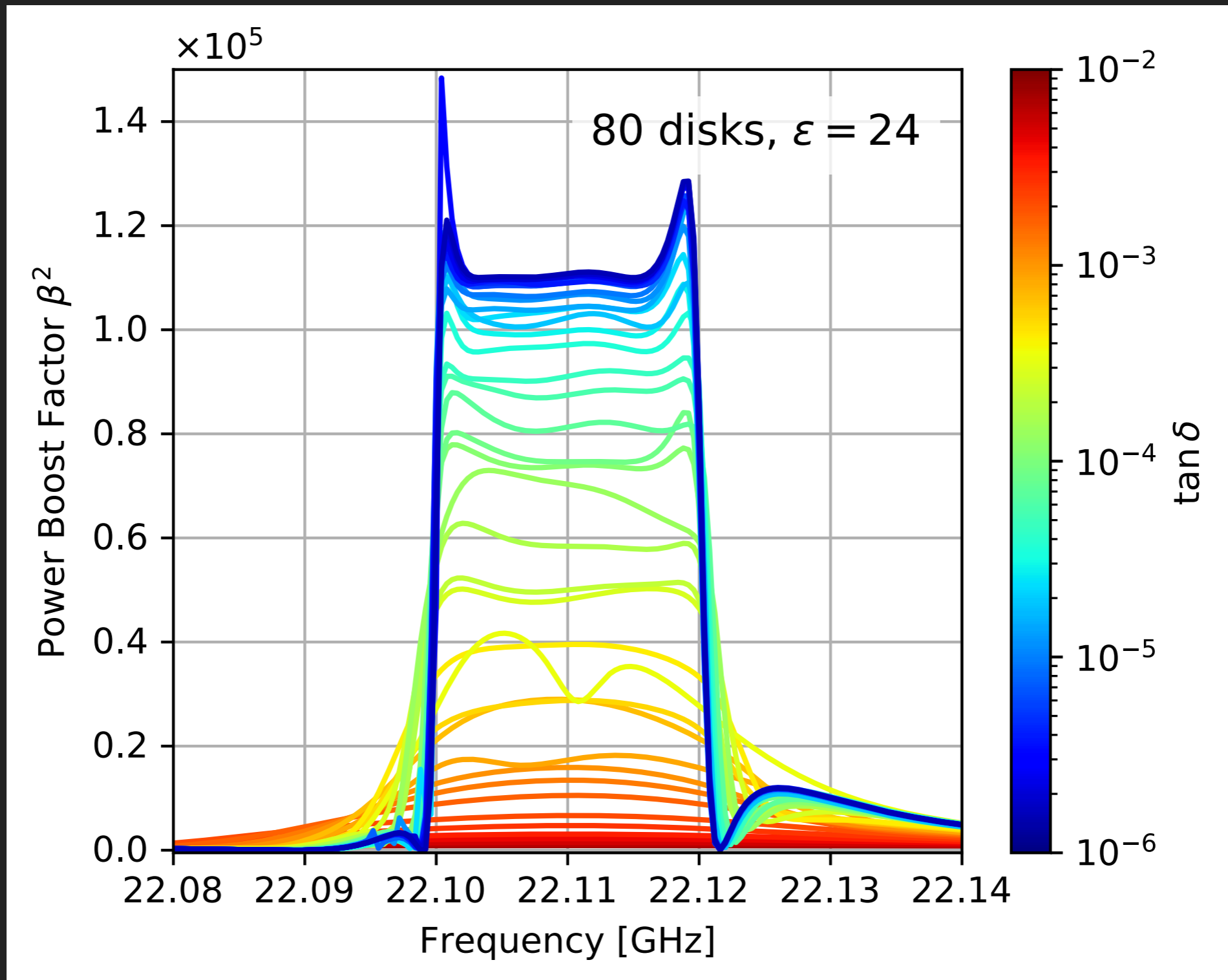
- ▶ Booster physics
 - ▶ Realistic simulations of axion signal and EM measurements
 - ▶ System noise temperature
 - ▶ Coupling of axion signal to receiver via antenna or taper
 - ▶ Other EM measurements to constrain boost factor?
- ▶ Frequency tuning of 80 discs
- ▶ Implementation of quantum limited amplifier below ~ 40 GHz
- ▶ Novel detection technology needed above ~ 40 GHz
- ▶ Engineering challenges
 - ▶ $100 \text{ T}^2\text{m}^2$ dipole magnet
 - ▶ Disc driving mechanism at 4K, 9 T, ~ 1 m driving distance, μm precision, 6 kg load bearing
 - ▶ Large dielectric discs with sufficient flatness, high ϵ , low $\tan \delta$



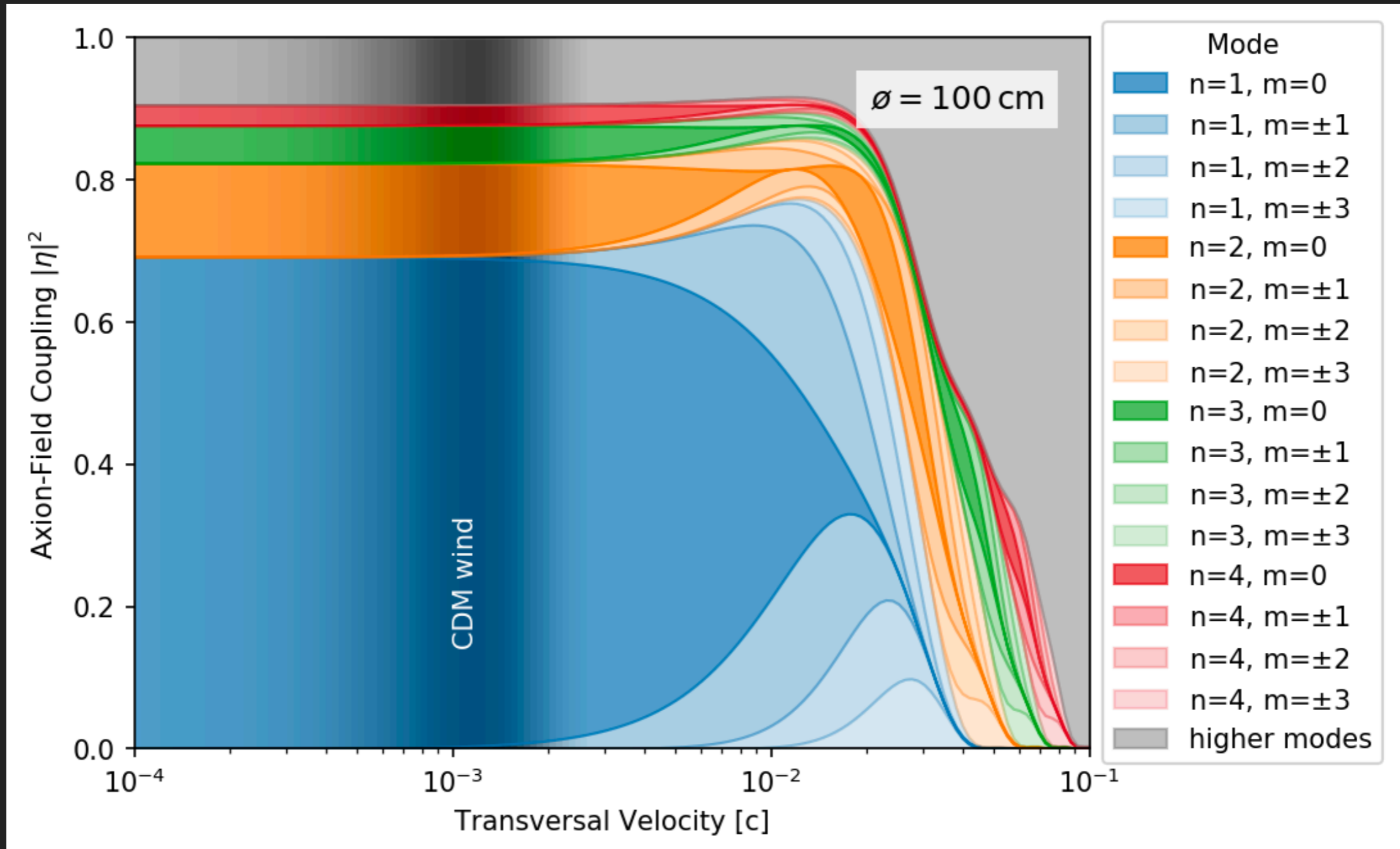
COLLABORATION



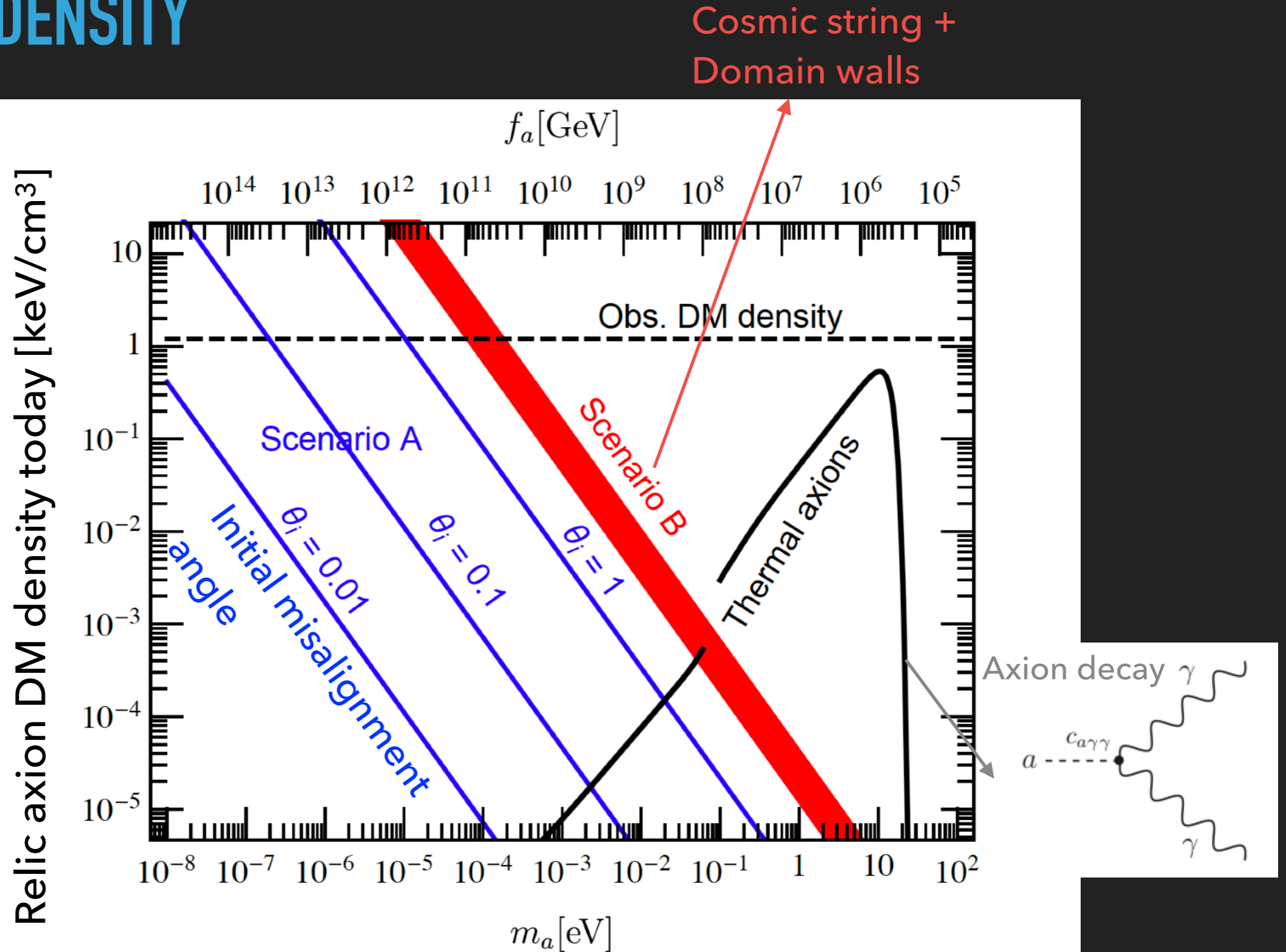
DIELECTRIC LOSS



AXION VELOCITY EFFECT



DM AXION DENSITY

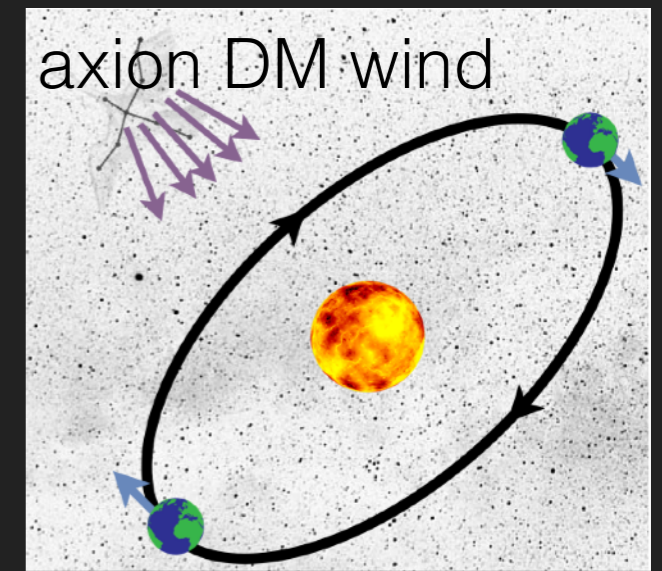


FROM AXION SEARCHES TO AN AXION TELESCOPE

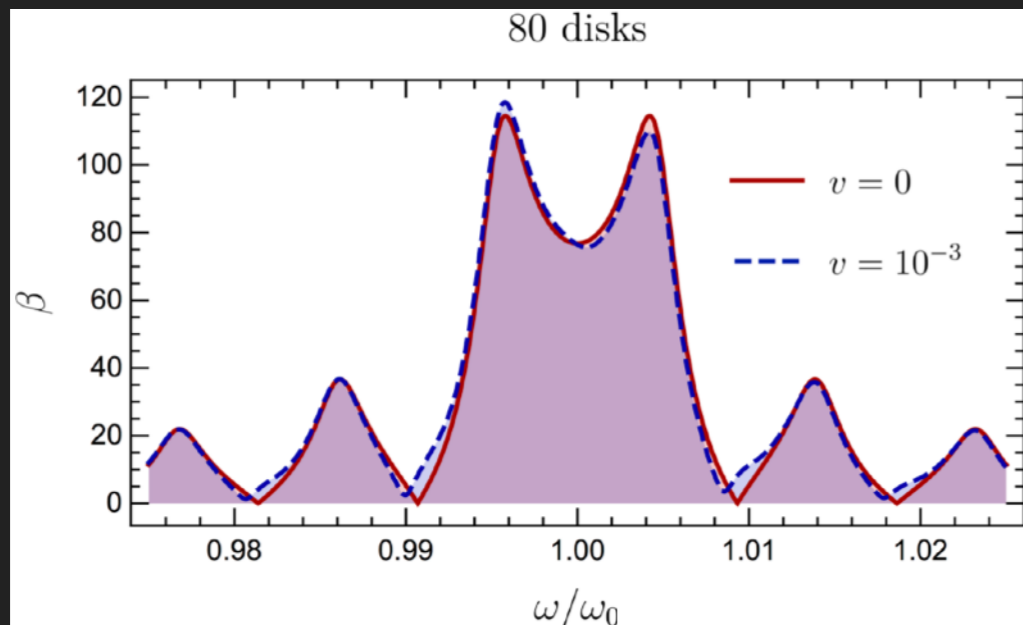
Axion DM field $a(\mathbf{x}, t) \approx \frac{\sqrt{2\rho_a}}{m_a} \cos(\omega t - \mathbf{p} \cdot \mathbf{x} + \alpha)$

$$\omega = m_a \left(1 + \frac{v^2}{2} \right)$$

$$\mathbf{p} = m_a \mathbf{v}$$

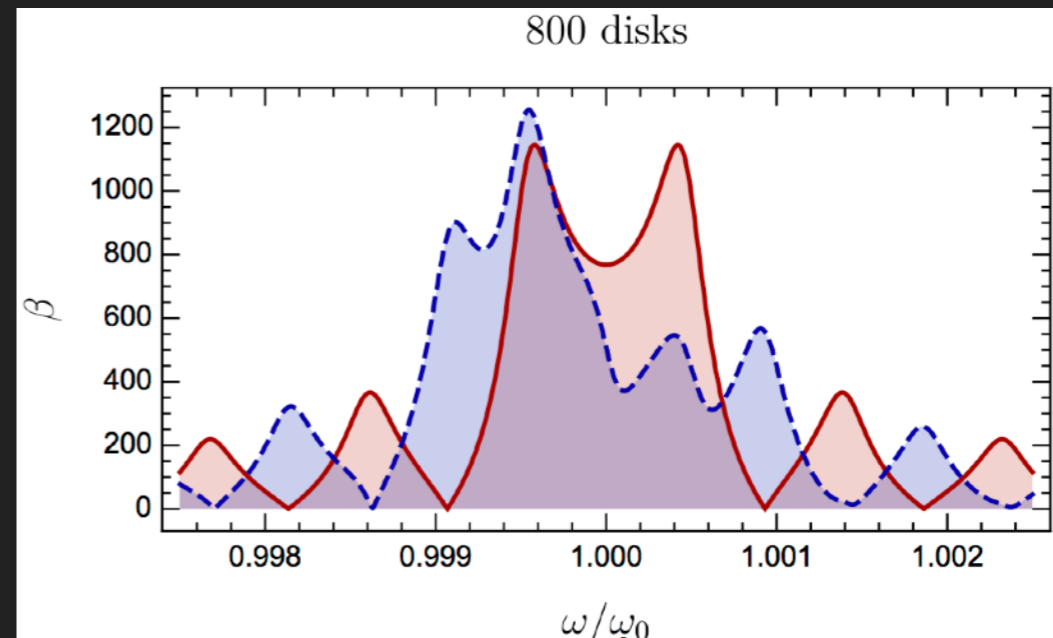


Axion search experiment



No v sensitivity

Axion telescope



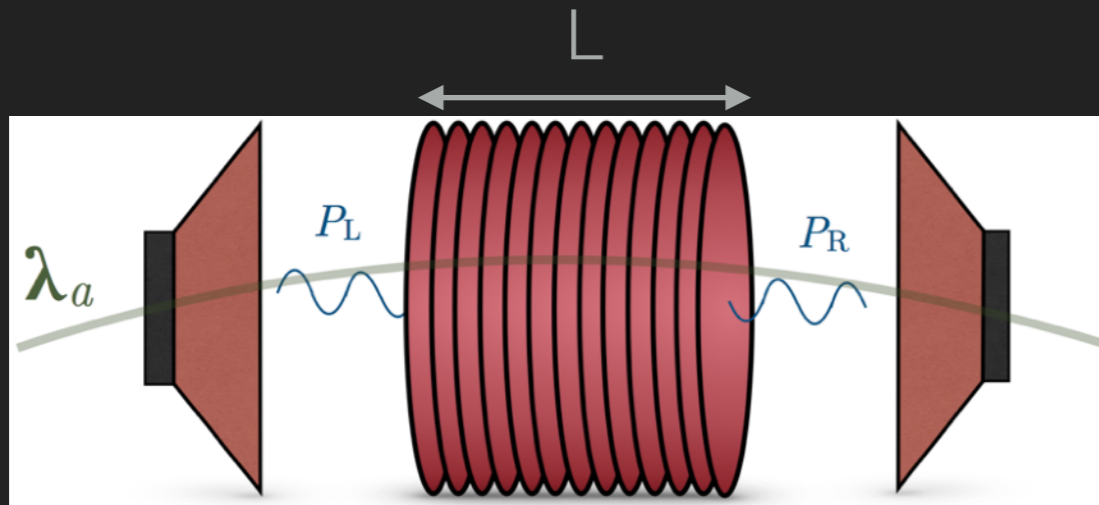
Directional v effect

A VISION FOR THE FAR FUTURE: AXION ASTRONOMY

Key: axion phase differences across large exp. + rotation of the Earth

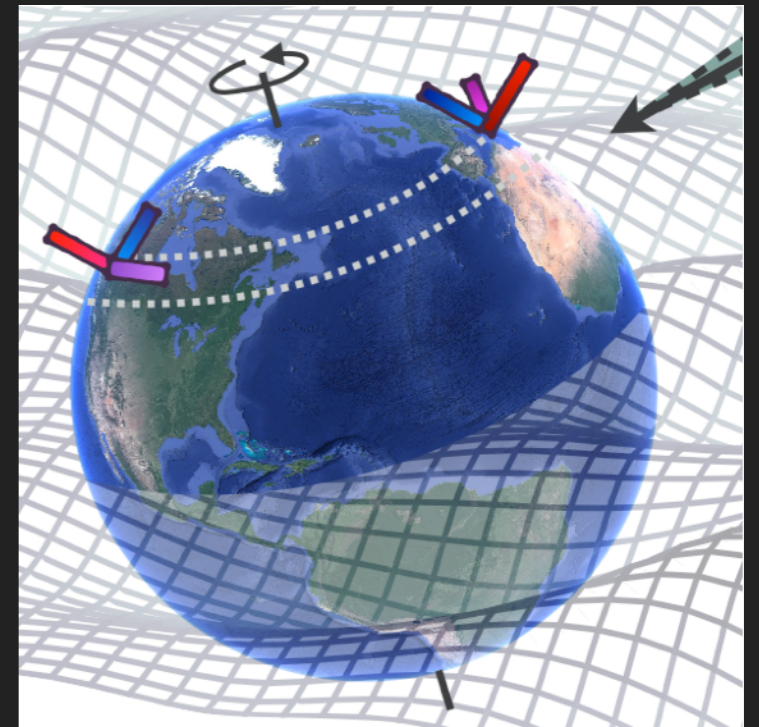
MADMAX-XXXL in 3 directions = axion telescope

Axion DM
wind



400 disks
 $B_e = 15 \text{ T}$
 $A = 1 \text{ m}^2$

$$L \sim \lambda_a = \frac{2\pi}{m_a \sigma_v} \simeq 12.4 \text{ m} \left(\frac{100 \mu\text{eV}}{m_a} \right)$$



- ▶ measure the daily and annual modulation (and solar velocity)
- ▶ measure the anisotropy of the DM halo
- ▶ measure a stream (and mini cluster streams)

[S.Knirck, A.J.Millar, C.A.J.O'Hare, J.Redondo, F.D.Steffen, JCAP1811, 051, arXiv:1806.05927]